Recent progress, challenges and outlook for multidisciplinary structural optimization of aircraft and aerial vehicles

G. Corrado[a,b], G. Ntourmas[b,c], M. Sferza[b,d], N. Traiforos[b,c], A. Arteiro[a], L. Brown[c], D. Chronopoulos[e,c], F. Daoud[f], F. Glock[b], J. Ninic[g], E. Ozcan[h], J. Reinoso[i], G. Schuhmacher[b], T. Turner[c]

[a] *DEMec, Faculdade de Engenharia, Universidade do Porto, Rua Dr. Roberto Frias, s/n, Porto, 4200-465, Portugal*
[b] *Stress Methods and Optimisation, Airbus Defence and Space GmbH, 85077 Manching, Germany*
[c] *Institute for Aerospace Technology & Composites Research Group, The University of Nottingham, NG7 2RD, UK*
[d] *Centre for Structural Engineering and Informatics, The University of Nottingham, NG7 2RD, UK*
[e] *KU Leuven, Department of Mechanical Engineering & Mecha(tro)nic System Dynamics (LMSD), 9000, Belgium*
[f] *Department of Aerospace and Geodesy, Technical University of Munich, 85521 Ottobrunn, Germany*
[g] *School of Engineering, The University of Birmingham, B15 2TT, UK*
[h] *Computational Optimization and Learning Lab, The University of Nottingham, NG7 2RD, UK*
[i] *Group of Elasticity and Strength of Materials, School of Engineering, University of Seville, Camino de los Descubrimientos s/n, 41092 Seville, Spain*

Abstract

Designing an airframe is a complex process as it requires knowledge from multiple disciplines such as aerodynamics, structural mechanics, manufacturing, flight dynamics, which individually lead to very different optimal designs. Furthermore, the growing use of Carbon Fibre Reinforced Plastics (CFRP), while allowing for more design freedom, has at the same time increased the complexity of the structural designers job. This has sparked the development of Multidisciplinary Design Optimization (MDO), a framework aimed at integrating intelligence from multiple disciplines in one optimal design. Initially employed as a tool to coordinate the work of several design teams over months, MDO is now becoming an integrated software procedure which has evolved over the decades and has become a prominent tool in modern design of aerostructures.

A modern challenge in airframe design is the early use of MDO, motivated by a pressing industrial need for an increased level of detail at the beginning of the design process, to minimize late setbacks in product development. Originally employed only during preliminary design, MDO has recently being pushed into early evaluation of conceptual designs with the outlook of becoming established in the conceptual stage. Using MDO during conceptual design is a promising way to address the paradox of design. By improving each concept, evaluating whether it is capable of meeting the design requirements and computing the sensitivities of various performance measures with respect to a design change, MDO enables designers to gain valuable knowledge in a design phase, in which most of the design freedom is still available.

We hereby exhibit the contemporary trends of MDO with specific focus on composite aircraft and aerial vehicles. We present the recent developments and current state-of-the-art, describing the contemporary challenges and requirements for innovation that are in the development process by academic and industrial researchers, as well as the challenges designers face in further improving the MDO workflow. Within the European OptiMACS project, we devised a novel holistic MDO approach to integrate a number of solutions to challenges identified as industrial technological gaps. These include two-stage optimization for layers of composites, addressing the presence of process-induced distortions and consideration of advanced failure criteria, including refined local models in early design stages, and seamlessly integrating software tools in the design process. The proposed methods are integrated and tested for structural case studies and the obtained results show the potential benefits of their integration into MDO tools.

Keywords: Multidisciplinary optimization, Aerostructures, Aerial vehicles, Manufacturing informed optimization, Aircraft composite structures

---

Contents

Email addresses: giuseppe.corrado@airbus.com (G. Corrado), georgios.ntourmas@airbus.com (G. Ntourmas), massimo.sferza@airbus.com (M. Sferza), neoklis.traiforos@airbus.com (N. Traiforos), aarteiro@fe.up.pt (A. Arteiro), louise.brown@nottingham.ac.uk (L. Brown), dimitrios.chronopoulos@kuleuven.be (D. Chronopoulos), fernass.daoud@tum.de (F. Daoud), florian.glock@airbus.com (F. Glock), j.ninic@bham.ac.uk (J. Ninic), ender.ozcan@nottingham.ac.uk (E. Ozcan), jreinoso@us.es (J. Reinoso), gerd.schuhmacher@airbus.com (G. Schuhmacher), thomas.turner@nottingham.ac.uk (T. Turner)

1. Introduction

The design optimization of aeronautical structures for sizing of primary structural components (wings, large portions of the fuselage) or even an entire aircraft is largely based on Multidisciplinary Design Optimization (MDO). Due to modern aircraft structures being largely made of advanced composite layered materials, in the design procedure the structural design parameters that have to be determined during the MDO has radically increased. For example, additional parameters to be determined as early as possible in the design process include the exact layering design of the structure (i.e. number, sequence, thickness and mechanical characteristics of each ply) and the manufacturing process to be followed for each component. The ensemble of the design variables has to be simultaneously considered and optimized vis-à-vis the adopted design criteria and constraints. In addition, composite structures require sophisticated numerical models with consideration of advanced failure criteria and description of the material at a mesoscale level, making the optimization process a computationally demanding task. Hence, there is a genuine industrial need for developing advanced MDO procedures that are able to reliably provide the optimal design of the composite structure under consideration within a rational amount of time.

As for any other complex product, the design of an aircraft structure starts with a list of requirements and desired product characteristics. At the beginning of the design process, engineers are free to make design assumptions, however at that stage they have limited knowledge on how these decisions will address the target requirements. As the design process advances, subsequent design decisions will always be constrained by the previous ones, which may result in failure to satisfy the requirements, and the designers will need to retrace their steps and redo the work (as illustrated in Fig. 1a). This problem is known as the *design process paradox* [1], where in the initial design steps (when the design freedom is maximal), there is a lack of information to guide the decision-making, while in the final design stages, when there is sufficient knowledge, the design freedom is minimal, as shown in Fig. 1b. Hence, considering the fact that the process of aircraft design is conducted in three stages (conceptual, preliminary and detailed) and across a number of departments, using computationally expensive numerical models, effective MDO procedures are required, preferably in early design stages, to gain more knowledge on structural performance ahead and allow for design flexibility without unnecessary repeated steps.

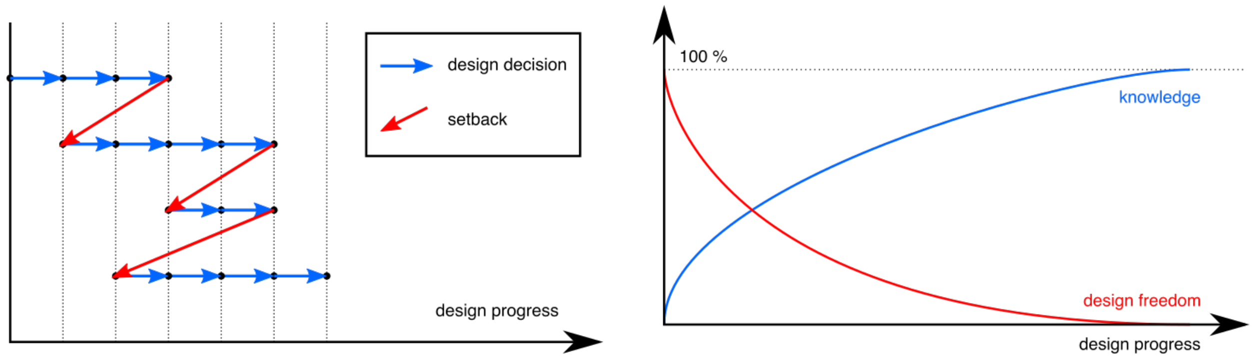

(a) Product development is characterized by steps forward and setbacks due to the violation of design requirements.

(b) The design paradox: as designers gain knowledge on how to design the product, they lose the freedom to modify the design.

Figure 1: Setbacks are normal in product development, but their opportunity cost increases as the design progresses, which leads to the design paradox.

A number of surveys have been published over the last two decades focusing on structural MDO with emphasis sometimes given towards mechanical analysis disciplines [3, 4], topology design considerations [5, 6] or optimization of stochastic parameters [7]. Literature reviews have also been provided towards computationally efficient schemes such as parallel architectures [8] or methodologies involving the employment of response surface (surrogates) [9]. Interest has also been rich considering optimization of geometrically complex architectures both regarding the mesoscale material design for composites [10, 11] and the macroscale geometric design at a component level [12–14].

Structural MDO has also been a topic of intense activity within the aeronautical industry. The need for lightweight and more efficient flying products has been steadily increasing over the last three decades given the rise in interest sourced from global travellers. Overarching survey reports have sporadically summarized the progress in aerospace MDO over time [15–18] with interest progressively shifting towards optimization of uncertain parameters [19, 20], as well as collaborative optimization [21, 22] specifically pertaining to complex structural areas [23]. Aeroelasticity is evidently a factor which can have radical impact on the structural design, with a few surveys [24–29] having been published regarding developments towards inclusion of aerodynamic and aeroelastic phenomena in the MDO framework. Before considering the comprehensive or even the preliminary aircraft structural design, MDO frameworks need to be able to determine optimal conceptual design choices for the vehicle. Hybrid electric architectures have been increasingly considered [30, 31], while blended wing body concepts [32] and wing morphing [33] are also design paths that need to be explored before reaching a decision. Inclusion of manufacturing constraints and uncertainty in the MDO process [34] is a topic which also received increasing interest, on which however few survey manuscripts have been published.

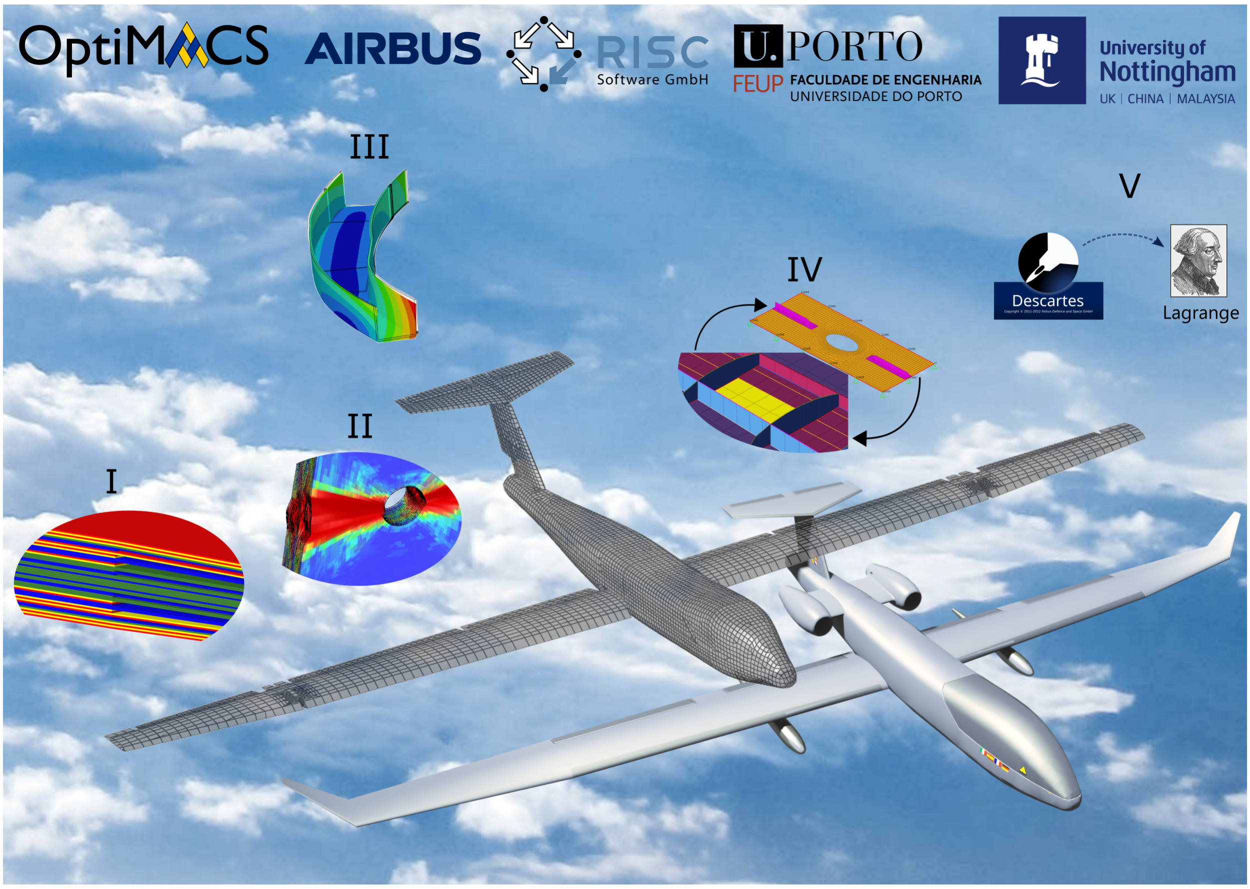

Figure 2: Contribution of each research topic explored in the Optimization of Multifunctional Aerospace Composite Structures (OptiMACS) project illustrated on OptiMALE [2], a Medium Altitude Long Endurance aircraft used as an academic demonstrator. In particular, these topics are: I) stacking sequence optimization; II) failure criteria and damage models; III) prediction of manufacturing distortions ; IV) global-local optimization; V) integration of software tools.

While MDO is to a certain extent still performed at a coarse resolution using low-fidelity models in a relatively manual process, the significant financial implications of the decisions made in the early design stages are putting an increased focus on achieving improved design accuracy, with a high degree of robustness. Specifically pertaining to the aerospace field, emphasis is therefore given to seamless integration of disciplines and a fine representation and resolution of geometric and material details wherever possible. New disciplines which were not explicitly accounted for until now (e.g. manufacturability and maintainability of a certain component) are also finding application within modern MDO frameworks.

A set of sophisticated software tools is currently employed within the European aerospace industry in order to perform structural optimization [35–37]. Such MDO platforms may have a number of design and performance optimization criteria implemented, with structural weight, structural strength, aerodynamic and aeroelastic performance disciplines being included amongst others. However, the number of computational and analysis stages performed through discrete software modules (i.e. the optimizer module, visualization and manual post-processing modules, design verification modules and design drawing and export modules) renders the modular data management a time consuming and counterproductive task. Taking into consideration the several thousands of design variables required for a large aerospace product, it becomes obvious that a genuine global industrial need exists for:

- Increasing the computational efficiency of the optimization models and algorithms currently employed in the aerospace MDO platforms.
- Developing seamless procedures for facilitating modular data interchange during the optimization process, and
- Extending the current set of adopted models and design criteria (also in view of the recent advances in the fields of manufacturing processes and numerical characterization of composite structures) in order to enhance the accuracy of the optimization process.

Motivated by these industrial needs, OptiMACS, a Marie-Curie research activity funded by the European commission, was coordinated in order to deliver the most cutting-edge research and training in the field of aerospace composite structures MDO through intense training of five early-stage researchers. During the work on OptiMACS, the Airbus in-house tools *Lagrange* and *Descartes* are used as a testbed to mature these new technologies:

- *Lagrange* is a multi-disciplinary structural optimization tool which has been continuously developed since 1984 and applied to the design of various military and civil aircraft. *Lagrange* consists of a general purpose finite element solver well suited to the thin walled stiffened structures used in aerospace, optimization algorithms and routines for evaluation of criteria models. Particular attention is paid to the modelling of composite structures. The unique aspects of *Lagrange*, however, when compared to commercial structural optimization codes, are the availability of the fully analytical sensitivities of each system response to a given set of design variables and the integration of diverse linear aerodynamic analysis tools for aeroelastic and loads analysis, including analytical sensitivity of aerodynamic and aeroelastic responses. This enables highly efficient gradient based search of the design space for the optimum design. Several optimization algorithms are implemented in the program to this end, each suited to a specific type of optimization problem. These include both, first and second order methods supporting a large number of design variables (approx. 10^5 - 10^6) and many constraints (approx. 10^6 - 10^8). The automation of both load analysis and structural sizing process is a key capability for the cost efficient development of high-performance flying aircraft. See [35] for further information.
- *Descartes* is a flexible parametric geometry builder and automatically generates a parametrised geometry model from an imported database in the Common Parametric Aircraft Configuration Schema (CPACS) format [38] which has been developed by the Deutsches Zentrum für Luft- und Raumfahrt - German Aerospace Center (DLR). The CPACS XML data and design language provides all necessary characteristics of an aircraft concept from one central database. The development of *Descartes* is based

on the TIVA Geometric Library (TIGL) , also from the DLR. *Descartes* can not only import CPACS data, but it provides also the GUI to create a new aircraft model from scratch based on engineering parameters. After the geometric model is set up, *Descartes* can derive a finite element model as well as aerodynamic analysis models and the coupling model (splining) between both. *Descartes* is intended for two major purposes. First, to support the conceptual aircraft design process with numerical analysis models, usually applied at the preliminary design phase, and second to enrich the Multidisciplinary Design Optimization (MDO) process with the prospects of a geometry kernel. Here, it can be used to morph the different analysis models during a shape optimization process. See [39] for further details.

Concurrently with the need for developing the appropriate technologies, there is also a need for exciting and motivating researchers regarding modern industrial technological gaps. This is the prime incentive for developing this manuscript focusing on recent developments pertaining MDO in Airbus, specifically within the frame of the OptiMACS project which was a Marie-Curie research activity funded by the European Commission. Fig. 2 shows schematically how each research work contributes to OptiMACS, where a novel holistic MDO approach is developed to enable the exploitation of the complementary competences of the researchers.

Structure of the manuscript. This paper is structured as follows: Sec. 2 gives a summary of several important open questions and challenges that industry practice is facing when using the currently available MDO procedures for optimization of aircraft structures with regard to MDO architectures, optimization criteria and constraints. Sec. 3 presents the proposed solutions developed within the OptiMACS project, addressing the practical challenges by means of i) an advanced solution for layer design optimization; ii) advanced failure criteria suitable for MDO processes; iii) consideration of Process Induced Distortions (PID) in the manufacturing procedure; iv) a novel global-local MDO procedure for early design with up-to-date local information in global models; and v) seamless integration of software tools and automation in the design process. Sec. 4 presents practical examples of how the proposed solutions have addressed the described practical challenges. Lastly, Sec. 5 concludes the paper.

2. Industrial challenges in aircraft conceptual design stage

2.1. Stacking sequence optimization of aircraft structures

Modern aircraft are increasingly using lightweight structures made of CFRP. For load carrying parts, the aeronautical industry relies mainly on continuous Unidirectional (UD) carbon fibres due to their superior mechanical properties, in particular high stiffness and strength, along the fibre direction compared to other forms of CFRP. The properties in the transverse direction are mainly dominated by the plastic matrix of the composite and thus such a UD material is highly orthotropic in nature. During production, UD plies, with a fixed thickness dependent on the sourced materials, are stacked on top of each other to form the required section of the part. This layered nature offers a huge design freedom. By varying the orientation of the fibre angle and the order of the different plies, the mechanical properties of the resulting laminate can be tailored to best suit the direction and scale of an applied loading as well as to meet extensional or flexural stiffness requirements.

This advantage comes with the price of significantly increased complexity, as large structures such as wing covers can be made of hundreds of single plies. What is more, the structural requirements of such large-scale components vary across their span and therefore different regions or patches of these components must be modelled with stacks of different thickness and composition while maintaining continuity or blending of the individual plies. The thickness difference across different patches is visible during the Automatic Tape Laying (ATL) manufacturing process employed for the component of Fig. 3. Additionally, manufacturing requirements and the avoidance of negative mechanical behaviours further constrain the task. These constraints influence either the stacking sequence of a laminate itself, e.g. by requiring a symmetric or balanced lay-up, or the transition between laminates, e.g. by restricting the maximum slope when ending multiple plies. A more complete list of these rules and the reasoning behind them can be found in relevant works [40–42]. It is worth noting that while some of these design rules are often relaxed in academic studies by using more sophisticated analysis [43–45] and manufacturing methods [46–48] the industry is following most of these rules to ensure robust processes and designs as well as simplifying and thus de-risking certification of the aircraft by using known and well understood principles.

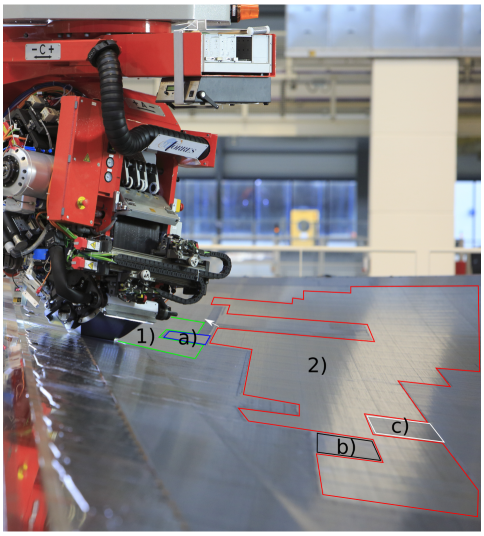

Figure 3: Visible skin patches formed by thickness differences across the span of the structure during the ATL manufacturing process of a wing cover.

The complexity in designing large CFRP structures therefore leads to surging development costs and a higher chance of errors when using a traditional development process. Therefore industry aims to mitigate this problem by applying optimization algorithms to find feasible designs [36, 49–52].

The main challenge linked with the stacking sequence optimization of large-scale aerospace structures is the mixed discrete and continuous nature of the problem. Structural constraints such as strength, buckling, maximum displacements, etc. are formulated using continuous quantities and depend on the solution of a FE-model which for large problems is significantly expensive in terms of computational effort. On the other hand, design and manufacturing rules concern discrete plies. The problem that arises is that different optimization algorithms are better suited to tackle different parts of the problem. Heuristic algorithms can be utilized to handle the discrete design variables and constraints however, such algorithms require a lot of iterations especially when the design variables increase which is prohibitive given the fact that physical constraints are linked with high computational expense. On the other hand, gradient-based algorithms are well suited for the physical constraints of the problem but do not perform well with its discrete characteristics.

This has led to two-stage approaches which first employ a gradient-based optimization algorithm to get a continuous thickness and stiffness distribution of the structure followed by a non gradient-based algorithm to handle the discrete requirements [53–55]. Unfortunately, a gap is inevitably created between these two optimization stages which in order to be bridged requires multiple iterations of the two-stage process, leading to a significant penalization in terms of performance metrics of the aircraft and also added effort by multiple design teams that have to repeat the process until a result fulfilling all structural and manufacturing requirements is retrieved.

2.2. Failure criteria for composite materials

To identify feasible solutions when computing the optimum design of an airframe, the corresponding optimization problem should account for different failure criteria among the structural constraints. Failure in aerospace composite structures, in fact, is a complex phenomenon which can occur due to different failure mechanisms: ply failure (where failure can take place in the matrix, fibre and fibre-matrix interface), delamination, global buckling, local buckling, crippling, column buckling, etc. The understanding of these phenomena gave an essential contribution to describe the performance envelopes of aerospace structures. Therefore, for the prediction of the onset of the mentioned failure mechanisms, as well as for their propagation, a countless number of failure criteria and progressive damage modelling approaches can be found in the literature. Recent reviews of these methodologies to address failure in composite materials can be found in [56, 57].

For the prediction of ply damage onset, failure theories are usually classified in two groups, by distinguishing theories that do not account for different failure modes, denoted as *non-phenomenological* failure criteria, and failure theories that are able to identify the different failure modes, denoted as *phenomenological* failure criteria [58, 59]. The first group comprises criteria in which a failure envelope is typically defined by using a single mathematical expression, usually a polynomial form, which predicts failure by interpolating between experimental data on simple (usually uniaxial) stress (or strain) states. Tsai-Wu and Tsai-Hill are two common examples of non-phenomenological failure theories. Failure criteria of the second family predict failure based on phenomenological considerations, by combining different theories to model the specific failure modes. Among the available phenomenological failure criteria, Hashin, Puck and LaRC failure theories can be highlighted.

The primary issue with including failure constraints directly in the structural optimization problem is its resulting size. Indeed, in a typical application of structural optimization, failure constraints may be enforced element-wise in the finite element model. However, for detailed, high-fidelity structural models, this can lead to an optimization problem with many thousands or millions of failure constraints, depending on the dimension of the model. These constraints are costly to enforce because they can only be checked by completing the structural analysis [60].

For the prediction of structural failure at the global level in MDO procedures, a commonly used failure criterion for MDO is the maximum strain criterion, because of the multi-step process used to determine the composite layup [61]. However, state-of-art approaches to ply failure onset have achieved a high degree of accuracy, being able to represent several relevant aspects of the failure process of laminated composites, e.g. the increase on apparent shear strength when applying moderate values of transverse compression, or the detrimental effect of the in-plane shear stresses in failure by fibre kinking. The most advanced set of phenomenological failure criteria account for the effect of ply thickness, fibre misalignment in compression, the effect of hydrostatic stresses and the effect of shear nonlinearity on fibre kinking, and the in-situ strengths [62–65].

The industrial challenge linked with failure criteria is to use advanced phenomenological failure theories to establish new laminate strength analysis models, suitable for optimization purposes. A validation study of the predictions against experimental results will be required, comparing the new model with the previous approaches in terms of reliability and efficiency.

Alongside the challenges in the deterministic methods, a recent effort has been made to enhance the reliability of aerospace vehicles and decrease the chance of failure under potential critical condition, by the development of non-deterministic approaches for optimization problems. In general two categories of uncertainty-based design methods can be distinguished: reliability-based design optimization (Reliability-Based Design Optimization (RBDO)) and robust design optimization (Robust Design Optimization (RDO)). RBDO allows to formulate the probability of failure in the optimization problem. The aim of this approach is to reduce the inherent conservatism of constant safety factors, which cannot weight the potential uncertainties. However, for large-scale, highly non-linear, and non-convex problems, the deterministic MDO is already challenging and it naturally requires prohibitive computational power to deal with uncertainties [16, 66]. For this reason, non-deterministic approaches are not included in the industrial challenges of OptiMACS.

In the previous sections, the importance of increasing the level of accuracy in modern MDO procedures from early stages of the design was highlighted. Global-local techniques can represent a suitable answer to this challenge, thanks to their ability to capture the behaviour of non-regular areas through local detailed models. Since this improved representation comes at a reduced computational cost due to the local refinement, this approach is of great interest for the aerospace industry. For instance, the structural sizing could benefit from detailed models, where critical load cases can be correctly analysed.

Recently, few global-local procedures have been proposed to predict the global ply failure and local skin-stiffener debonding of reinforced panels, while reducing the computational time [56, 67, 68]. In particular, these methods proved to be reliable and efficient tools to study localized nonlinearities, such as onset and evolution of damage, minimizing the computational effort. For instance, a two-way coupling global-local approach, described in [68], enabled to address delamination phenomena through a local analysis based on cohesive elements and to ensure that the energy dissipated due to delamination evolution at the local level was captured at the global level, with special attention to the exchange of information between the global and local models. The validation of this method established a reliable procedure of dissipated energy calculation for the global model due to delamination based on the dissipated energy in the local model.

However, so far, only delamination has been properly addressed into these global-local frameworks. For this reason, an additional challenge for OptiMACS is to tackle the integration of ply damage into an efficient global-local Finite Element (FE) approach.

2.3. Prediction and compensation of distortions induced in composite structures by their manufacturing processes

The challenge in the manufacturing industry is to achieve a "First Time Right" approach in order to increase product quality and reduce manufacturing costs and delays related to manufacturing defects. In order to do so, in the manufacturing of composite structures it is very important to monitor and minimize Process Induced Distortions (PID).

PID are the result of the combined effect of composite warpage and spring-in and can be attributed to the residual stresses which are imposed within the structure during its manufacture [69]. Almost every composite structure suffers from this manufacturing defect to some degree.

Therefore, a tolerance range is set for each composite part within the structure to be manufactured. This will not only increase the structural performance of the part due to the reduction of the respective residual stresses, but will also ease the assembly process, reduce the assembly time and costs. If the structure is outside of the tolerance range it is scrapped and the tool which has produced the part has to be modified - if not completely redesigned - to produce the desired geometry. In some cases, the design (geometry, materials, or layup strategy) of the final product has to be reconsidered in order to reduce its shape distortions after manufacturing.

Fig. 4 depicts what it is done currently in the industry to compensate for PID in the design of new moulds.

The challenges to be addressed in the design process of moulds for composite structures are :

- To increase material modelling accuracy (Step 2 & 4 in the design process as depicted in Fig. 4)
    - Investigation of advanced material models (viscoelastic vs elastic or modified elastic models)

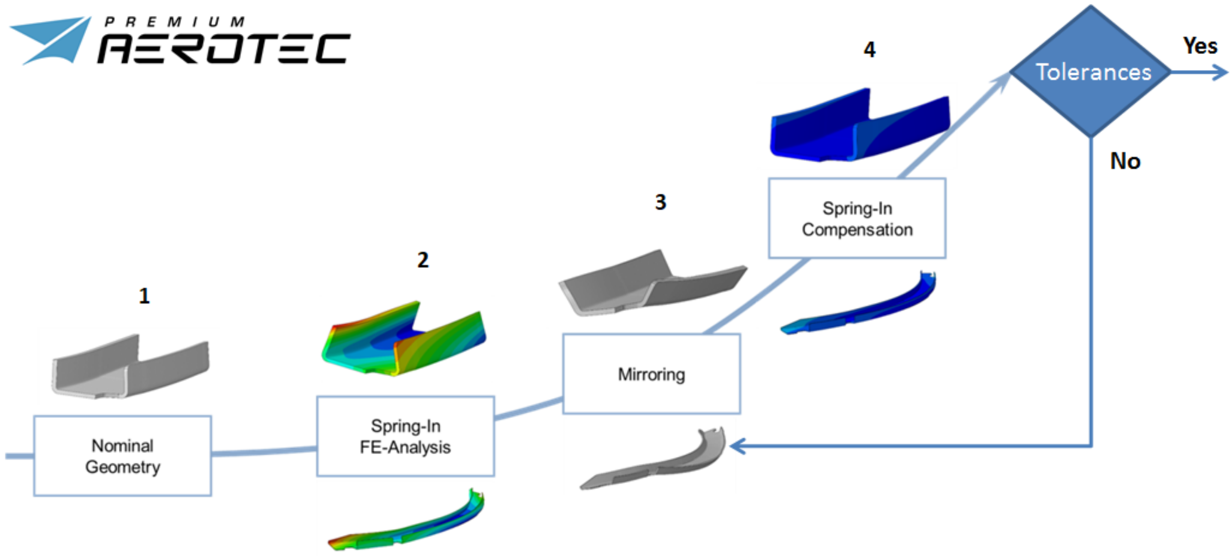

Figure 4: Design approach to produce the compensated mould geometry [70].

  - Couple the material models with advanced functionalities (tool-part interaction, heat transfer analysis, chemical shrinkage strains calculation)
  - Investigate different boundary conditions and their effect on simulation results.

- Automate the mirroring process for mould compensation (Step 3 in the design process as depicted in Fig. 4). The motivation here is to give the stress engineers all the tools they need to perform spring-in analysis without interfering with other departments (CAD, etc.) which is a time consuming and costly process especially in big companies.

- Experimentally validate the developed spring-in simulation framework. For the material system under investigation assess the simulation framework accuracy in academic and industrial parts. Identify sources of potential error to improve either the modelling or the manufacturing side of the structure.

2.4. Global-local multidisciplinary optimization of airframe structures

Traditionally, multidisciplinary structural optimization of aircraft employs coarse FE-models often combined with analytical post-processing to compute e.g. plate stability using stresses from the linear Finite Element Method (FEM). This implies that local areas with complex structures or load concentrations are idealized in a simplified manner which does not capture all effects. Hence this representation rarely provides enough information to analyse this area sufficiently during early design phases and it is hardly ever appropriate for sensitivity analyses. Frequently, the stiffness of these local areas is estimated by simple methods and engineering judgement and the region is fixed during the optimization. However, if this manual step is not sufficiently accurate, designers may be forced to accept sub-optimal local solutions or require global changes at a later stage. Especially these late changes in the global design lead to setbacks and are hard to recover. Therefore, a general trend in the industry to include more details in preliminary design can be seen [36, 37]. This is especially true in the context of MDO where the fidelity level at the system level is determined by the discipline with the lowest-fidelity model [71]. Additionally, this lack of information limits the ability of designers to compare different concepts during the very early stages, since the data regarding predicted performance is inaccurate [72].

While it becomes clear that it is necessary to include such details in early design stages, the performance is crucial when analysing a complete aircraft or large components in a multidisciplinary optimization. This prohibits refinement of the full model and thus it makes sense to employ so-called global-local techniques [73–80]. The non-regular local area is idealized with a refined model which allows capture of all relevant effects and size this area. Reduction methods such as [81] can be used to obtain accurate, but reduced stiffness and mass matrices which will be used in the global model. The global model itself is rather coarse, but sufficient to represent the overall stiffness and mass and allows the sizing of regular areas, while having reasonable computational cost. At system level, only the global model is used for studies of aeroelastic tailoring, flutter analysis, etc., while the local model might only be used during the structural sizing and could even be skipped for loadcases known not to be design-driving for this area. This allows avoidance of excessive computational cost, while capturing the necessary information. A further challenge is to select an appropriate architecture for the MDO process which is able to exchange and use the information relevant to the analysis such as mass and stiffness properties, but also sensitivities with regards to the design variables and the corresponding displacement field.

2.5. Integration

Evaluation of airframe design requires cooperation and transfer of information between teams working on different stages of the design process. The multidisciplinary design team add structural and aerodynamic details to an initial airframe design created by the conceptual design team. The performance of this more detailed design is then evaluated based on the desired objectives and metrics. This is a process which is time-consuming and which currently requires manual transfer of data between the different software packages used during the process as shown in Fig. 5. This figure illustrates the workflow from the initial airframe design in CPACS format [38] to model generation using *Descartes* [39] and finally optimization using *Lagrange* [35]. The blue rectangles in the figure highlight where manual transfer of data is currently required with the consequence that the current workflow to evaluate the performance of a single airframe design may take one to two months.

Due to the manual nature of the data transfer interfaces, the length of time for airframe evaluation is currently a barrier to the ability to perform any optimization for the overall airframe design. Automation of these interfaces will make the use of MDO feasible for the exploration of multiple airframe design variations.

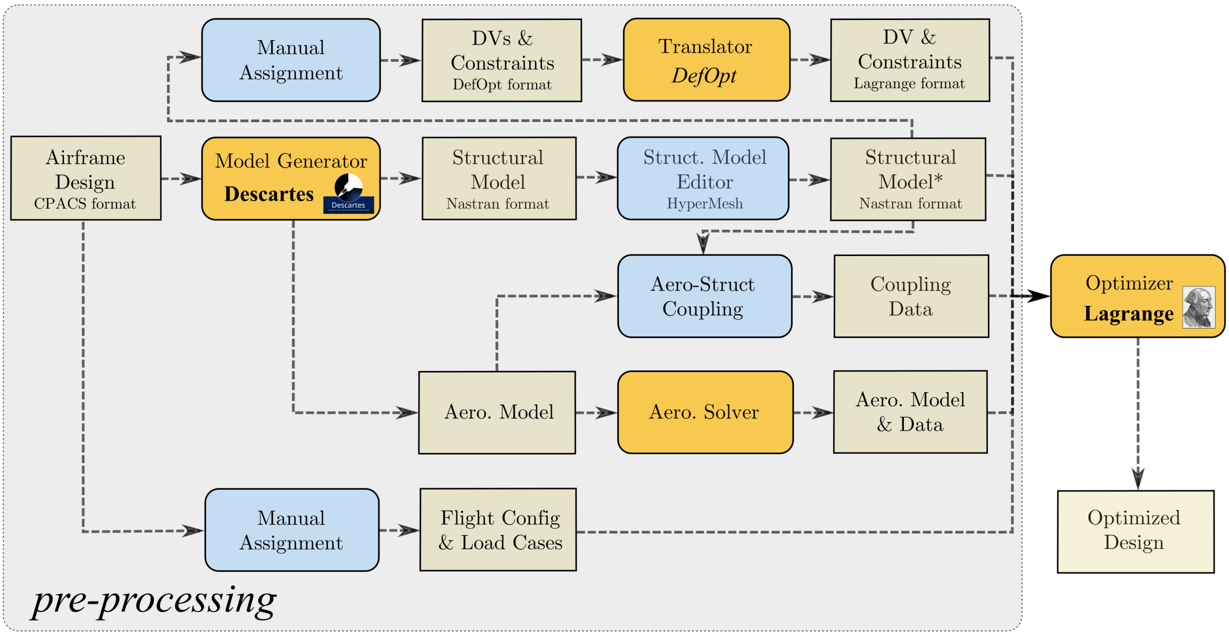

Figure 5: Current airframe design performance evaluation workflow. The airframe design (in CPACS data format) flows from the model generator (*Descartes*) and computation of input data (within the "pre-processing" box) to the optimizer (*Lagrange*) in order to obtain the final optimized design.

3. OptiMACS contributions

3.1. Stacking sequence optimization

As discussed in Sec. 2.1, two-stage optimization approaches offer the most potential for successfully deriving discrete stacking sequences for aeronautical structures. In the framework of the OptiMACS project, a two-stage optimization has also been adopted to perform the optimization task. In contrast to other approaches employing lamination [53, 82, 83] or polar [55, 84] parameters to model the thickness and stiffness of the structure in the first, gradient-based stage of the optimization, the methodology adopted within *Lagrange* uses generic stacks to model the properties of the structure. A generic stack is composed of multiple generic layers whose exact orientation and stacking sequence is fixed during the optimization. Therefore, the design variables employed during the optimization correspond to the individual thickness of each generic layer, which can take any real positive value. In the most simple case demonstrated in the optimization flowchart of Fig. 6, each generic stack models one patch of the structure and only comprises 8 generic layers. In other words, the generic stack used is $[45, -45, 90, 0]_s$. If symmetry of the laminated structure was also enforced in the optimization study, then this would lead to 4 design variables, while if balanced laminates were additionally required, only 3 design variables per patch would be needed for this simple generic stack. In practice, generic stacks with at least 16 generic layers should be used in order to achieve an adequate representation of the stiffness design space. The number of plies and stacking sequence of the generic stack need to be chosen so that the resulting thickness and stiffness do not depend on the modelling decisions in the part. More guidelines on these modelling decisions have already been discussed in previously published work by some of the authors [85], and it has been shown that a reduced number of design variables can adequately model even thick industrial-scale structures.

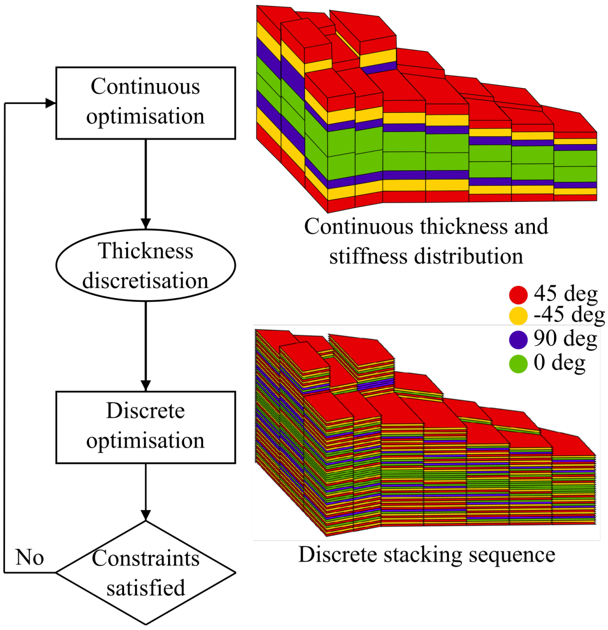

Figure 6: Flowchart of the two-stage stacking sequence optimization process.

The optimum continuous solution computed by the gradient-based optimization needs to be translated into a discrete stacking sequence which satisfies all the composite design and manufacturing rules. Since the thickness of the pre-impregnated tape that will be used for manufacturing is known, the entire thickness of each generic stack is rounded-up to either the nearest integer number of plies or the nearest even number of plies. This discrete number of layers for each patch remains constant during the discrete optimization.

The second stage of the optimization involves mathematical programming and solving a Mixed Integer Linear Programming (MILP) formulation of the stacking sequence optimization subject to any composite rule, aiming to match the stiffness characteristics derived in the first stage as accurately as possible. Two equivalent formulations of the stacking sequence optimization problem subject to various composite design and manufacturing rules have been derived [42]. These MILP formulations offer more design freedom than most available blending representations [41, 86, 87] and also achieve a more robust convergence towards the global optimum compared to heuristics. A decomposition technique which renders the optimization algorithm a heuristic one has also been developed to assist with the discovery of good local optima in a much shorter time frame for industrial-scale problems. The quality of these local optima may be adequate enough, rendering the search for a global minimum to the problem unnecessary. If this is not the case, the local optima can be used to initialize the non-decomposed formulation of the problem to enable faster overall convergence of the optimization.

The proposed two-stage optimization can consistently lead to discrete stacking sequences which satisfy all required structural constraints in only one pass of the two-stage process. This is mainly due to the fact that the design space of generic stacks allows for more composite rules to be implemented, since it is a direct representation of the sequence characteristics of the stacks. Moreover, the formulation of blending, in particular, is exact, compared to other approximate formulations when using other modelling approaches, such as lamination [54] and polar [88] parameters. As a result, the gap which is inevitably formed between the two optimization stages is bridged and the entire design process is simplified and accelerated. Moreover, by bridging this gap, the current methodology is able to achieve a lower structural mass when applied to a benchmark problem [85] compared to other studies sharing equivalent design criteria.

3.2. Integration of failure criteria in the MDO process

In Sec. 2.2, the challenges linked with the integration of failure constraints in large structural optimization problems were described. Additionally, another objective of this research work is to tackle the integration of ply damage and delamination into efficient global-local procedures. In the next sections, the methodologies implemented to address these research topics are described in detail.

3.2.1. Failure constraints in strain space for global MDO problems

Strength constraints suitable for MDO are required to outline safe failure envelopes for different loading conditions that do not compromise the efficiency of the optimization process. Another desirable aspect regarding failure criteria for MDO is their formulation in strain space, mainly because they can benefit from invariant laminate failure predictions with respect to ply orientations, simplifying the design of composite laminates. In fact, the failure envelope for a given ply angle is fixed in strain space independently of the orientation of the other plies in the laminate, unlike ply failure envelopes in stress space [89]. This means that these envelopes, as well as the inner failure envelope in strain space of a multi-directional laminate, can be viewed as material properties [90]. Failure envelopes in strain space, therefore, enable an invariant description of failure with respect to the ply orientation, which is essential for a continuous optimization with lamination parameters [91, 92], and to quickly compare against the maximum allowables obtained experimentally.

The challenge of this research work was to develop a laminate strength analysis method using an advanced phenomenological failure theory. To tackle this challenge, an extended failure prediction approach, based on a recently introduced concept called omni strain failure envelope [90, 93], was developed in order to address laminate failure under general 3D stress states and to identify critical failure modes [94]. A omni strain envelope is an envelope obtained by superposing failure envelopes for all possible ply orientation in strain space and extracting the inner design space. In fact, in strain space it is possible to superimpose the failure envelopes for the different ply orientations and compute a laminate failure envelope. This theory was originally proposed using the Tsai-Wu failure criterion applied at the ply level. With this approach, all laminate data can be displayed on one graph in strain space, realizing a very concise display of the strength of a given composite material. Furthermore, it is a very practical tool, enabling a fast selection of the stacking sequence according to the required mechanical properties, since it covers all the possible ply orientations.

Because the omni First-ply failure (FPF) envelopes represent the most conservative design solution, where all the plies remain undamaged, Tsai and Melo [93] proposed an extended version of this criterion, to define and predict the continued load-carrying capability of any laminate, after damage initiation. They introduced the omni Last-ply failure (LPF) envelope, which is an extension of the concept of omni FPF envelope to ultimate failure. The construction of these envelopes follows the same procedure as described before, but with degraded ply properties, based on a matrix degradation factor and micro-mechanics relations. Moreover, Tsai and Melo [93] observed that, for all CFRP laminates, the inner LPF envelope is controlled by the 0° and 90° plies loaded along the respective fibre direction.

Based on these observations, a further simplification of the failure analysis was performed introducing the unit circle failure envelopes for CFRPs in normalized principal strain space, which rely on just two strength properties: the longitudinal tensile and compressive strains-to-failure. Comparing the omni strain LPF envelope and the unit circle failure envelope of the same material, the unit circle envelope is inscribed in the omni LPF envelope. Although the failure predictions related with this criterion are intentionally conservative, this theory is extremely useful due to its simplicity. In particular, by requiring only the strains-to-failure of a 0° coupon measured in tension and in compression instead of complete characterization of the ply properties, not only the failure predictions, but also the material characterization can be substantially simplified.

By exploiting the fully 3D description of failure provided by the invariant-based theory proposed in [65], omni strain failure envelopes can be extended to omni strain failure surfaces by finding the controlling plies in the 3D principal strain space. Indeed, with this extension, the resulting design space can predict failure under complex 3D stress states of any laminate, independently of lay-up or stacking sequence, and address, for instance, the design of bolted joints or thick composite laminates, where through-thickness stress states cannot be neglected. Furthermore, in this case, the envelopes allow the identification of the critical failure modes for each controlling ply, which cannot be investigated with the Tsai-Wu based omni strain envelopes. An illustration of this extension of omni failure criteria is provided in Fig. 7, while a detailed presentation of this work is provided in [94].

It is also important to note that, for typical CFRP laminates, such as aerospace industry-standard "quad" laminates, characterized by different percentage of 0°, ±45° and 90° plies [95], omni LPF and laminate LPF envelopes (the latter obtained from superposing in strain space only the envelopes of the ply orientations contained in the selected laminate) will lead to the same laminate failure predictions. This is justified by the presence of the [0] and [90] plies in these laminates, which will govern LPF according to both approaches. Therefore, for all CFRP "quad" laminates, the omni LPF envelopes ensure the same degree of conservatism as the laminate LPF envelopes, but without the need to recompute the failure envelope every time the layup changes. However, when tackling LPF of angle-ply or double angle-ply (double-double [95]) laminates, omni LPF envelopes will have a certain degree of conservatism that will depend on the ply angles.

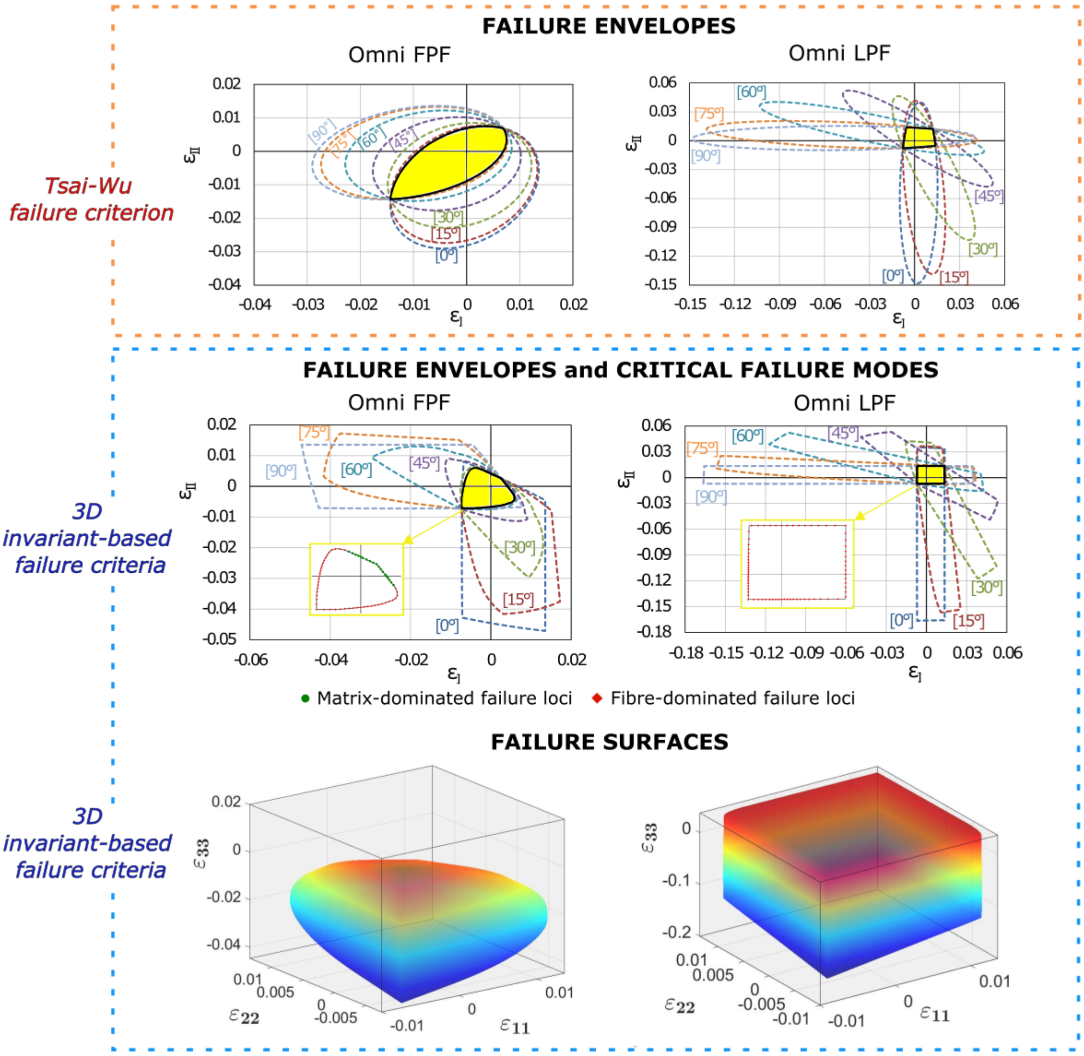

Figure 7: Omni strain failure envelopes and surfaces.

564 *3.2.2. Detailed progressive failure analysis for local models*

Global-local analysis is typically performed at the subcomponent level to address critical phenomena with detailed models and to translate the obtained results into the global scale. In this framework, failure criteria can be firstly implemented in the global level for "hot spot" identification to provide a first indication of the critical locations where detailed local analysis should be performed.

The implementation of failure criteria in a FE software for hot-spot failure analysis has been recently proposed in [96–98]. Exploiting the indications obtained from a hot-spot failure analysis, it is possible to increase the modelling resolution only where required, enabling a more efficient and reliable global-local analysis, especially when addressing large-scale composite structures. Molker et al. [96] proposed the implementation of LaRC05 for the prediction of failure initiation and critical failure modes of laminated composite structures, while a novel LaRC05-based failure theory was implemented to address damage onset of Non-Crimp Fabric (NCF) reinforced composites [98]. These implementations were done in the commercial FE code Abaqus/Standard, by means of a user defined subroutine UVARM creating element output variables at each integration point and each time increment.

As part of the OptiMACS project, the 3D invariant-based failure theory [65] is used for the prediction of FPF of laminated composite structures. With this aim, the formulation of this set of criteria was implemented in a post-processing Python script, compatible with Abaqus/Standard and Abaqus/Explicit, to generate new element output fields, by using the full stress tensor of each element and computing the failure index for each of the failure modes tackled by the criteria. Because of the fully 3D nature of the implemented failure theory, this approach allows the identification of "hot-spots" and the corresponding failure mechanisms for damage initiation, creating different output variables to predict fibre and matrix failure, under tension and compression. On the other hand, when the aim is to address LPF at laminate level, a model with an equivalent single layer discretization and a laminate failure criterion should be used, which is particularly interesting in large-scale structural models. With this purpose, an additional post-processing script is in place to compute and show the failure index obtained with unit circle failure theory [93], by means of an element output variable.

After identifying the "hot-spots" for the onset of ply or laminate failure, a detailed damage model can be employed to predict ultimate strength of the most critical areas, while representing all damage modes and their interactions. The damage modes taking place in composite materials evolve in various combinations that depend, among other factors, on the stacking sequence and ply thickness. Some combinations of damage may reduce local stress concentrations, while others may cause structural collapse. This is the reason why it is crucial to have a model that is able to predict damage initiation and propagation accurately [99].

Among the different scales of idealization of the damage process, which may span from molecular dynamics to structural mechanics, Fibre-reinforced polymers (FRPs) are most commonly represented at the mesoscale, due to the flexibility it provides in representing in detail the initiation and propagation of the different failure modes observed in FRPs within a reasonable computational effort. Mesoscale numerical models have been recently developed to represent the onset and broadening of the intralaminar damage modes (e.g., transverse matrix cracking and fibre failure) and use cohesive zone models to capture delamination between ply interfaces [100, 101].

The methodology introduced in this work consists of a composite material model proposed in the literature [101], representing the quasi-brittle behaviour of composite structures. It is extended to account for the effect of general 3D stress states in the initiation and broadening of fibre kinking using the 3D invariant-based failure theory, as described in [65]. The invariant-based failure criteria are coupled with a smeared crack model for transverse cracking and continuum damage mechanics models for fibre-dominated damage, which together account for the kinematics of matrix cracking and fibre tensile or compressive fracture during damage propagation. Furthermore, to predict delamination, cohesive elements are used at the interfaces between layers with different orientation. It should be noted that, to use cohesive zone models properly, a minimum number of elements within the cohesive zone is required. A quantitative study on this topic can be found in [102], where a procedure to use coarser FE meshes is described, identifying a minimum of 3 elements within the length of the cohesive zone to predict delamination growth without losing accuracy in the results.

3.3. Consideration of PID in the manufacturing of composite structures

To address the industrial challenges presented in 2.3 regarding the presence of Process Induced Distortions (PID) in the manufacturing of composite structures the OptiMACS project focused on the investigation of two material models regarding their ability to accurately predict the shape of the manufactured part. With the use of these material models a simulation framework was developed, able to take into account the majority of the factors reported in the literature to affect PID such as resin chemical shrinkage, tool part interaction, temperature gradients, stress relaxation, etc. [103–108]. The validation of the simulation framework for the material system studied was done by experimental investigations in the laboratory as well as with the study of an industrial size composite test frame.

More specifically after obtaining the certified stacking sequence of the composite structure, being a product of MDO analysis, the job of the manufacturing engineer is to design the mould and the tools needed to manufacture the part according to its quality criteria, as well as determine the manufacturing process suitable to produce the part (resin infusion, resin transfer moulding, etc.) within the given budget and time. Because of the limited design freedom in the late design phase of composite structures, MDO is rarely employed to address the manufacturing defects arising from the manufacturing process selected. These manufacturing defects include, but are not limited to delamination, fibre wrinkling, fibre reorientation, fibre pull-out, increased void content, etc. and usually a multi-physics analysis approach coupled with experimental investigations and manufacturing experience is used to address them and optimize the manufacturing process [109–112].

PID is a significant problem encountered in the manufacturing process of composite structures irrespective of the manufacturing method used. To counteract this manufacturing defect the manufacturing engineer simulates the three dimensional shape distortions of the part and mirrors the distortions to the mould by reversing the calculated part distortions in the opposite direction (Fig. 4). This approach is referred to in the industry as the mould compensation approach since the shape of the mould is different from the shape of the part that is going to be manufactured from it. The final product after demoulding will distort and if the calculations of the manufacturing engineer are correct, it will be close to its nominal geometry (Fig. 8).

The material model employed by the manufacturing engineer in this process is very important to accurately predict shape distortions. Three types of material modes are used with increasing complexity and accuracy: elastic, modified elastic and viscoelastic material models. The elastic material models focus on the development of the shape distortions of the structure during the cool down phase of the curing cycle, when the structure has attained its final degree of cure, and consider the material as elastic during this phase. On the other hand, the modified elastic models separate the curing history into a number of segments to which they assign an elastic modulus, in order to calculate the residual stresses and distortions

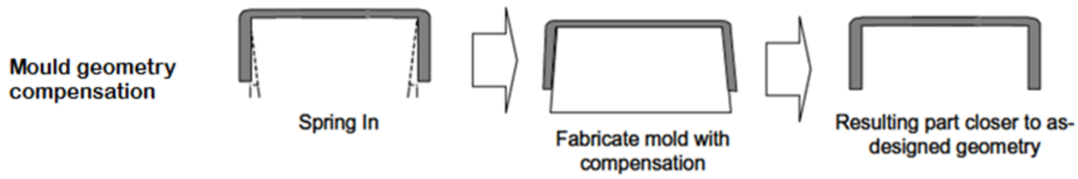

Figure 8: Mould compensation approach [113].The spring-in angle of the part is known a priori either through manufacturing experience or simulation. Therefore, the mould of the part is compensated accordingly (usually by mirroring the expected distortion of the part to the opposite direction) in order for the resulting part after demoulding to be closer to the as-designed (nominal) geometry.

of the structure. The viscoelastic material models are time depended models able to take into account the stress relaxation of the material during the cure and are regarded by the literature as more accurate compared to the elastic or modified elastic models or the use of analytical equations [114–116].

In the context of the OptiMACS project the Cure Hardening Instantaneous Linear Elastic (CHILE) material model was investigated. The CHILE material model is a simple, robust and fast model used by the academia as well as by industry to calculate PID of composite structures. However, since it is not a time dependent model it cannot take into account stress relaxation which occurs during the curing. The second material model investigated in the context of the OptiMACS project is the linear viscoelastic model proposed by Poon and Ahmad [117].

To exploit the full capabilities of the material models these were coupled with functions that calculate at each time step the resin chemical contraction, glass transition temperature, resin coefficient of thermal expansion, resin instantaneous fibre volume fraction and Poisson's ratio before employing the ply homogenization equations proposed by Bogetti [118] as depicted for the case of UMAT subroutine in Fig. 9 employed for the chemo-mechanical spring-in analysis.

To further increase the accuracy of the simulation framework developed, tool part interaction was studied in comparison to free-standing and fixed boundary conditions. Free-standing boundary conditions imply that the 3-2-1 principle is used to suppress rigid body motion of the part during the curing. At the fixed boundary condition the Degrees of Freedom (DOFs) 1,2 and 3 of the part are set equal to zero and as a result of the part not being able to move during the curing cycle.

Regarding the study of tool part interaction, a Coulomb friction approach was used in the context of the OptiMACS project. In the normal direction of the contact, "hard" contact was assumed meaning that the tool and the part could not penetrate each other. In the tangential direction a cure dependent Coefficient of Friction (CoF) was assumed from the gelation point to cool down. Instead of performing an experimental investigation to assess the evolution of coefficient of friction from the gelation point to cool down for the material system under investigation, a linear relationship was adopted from the literature [119].

The motivation for the development of a robust friction model to describe the forces that are transmitted from the mould to the part during the manufacturing cycle is to substitute

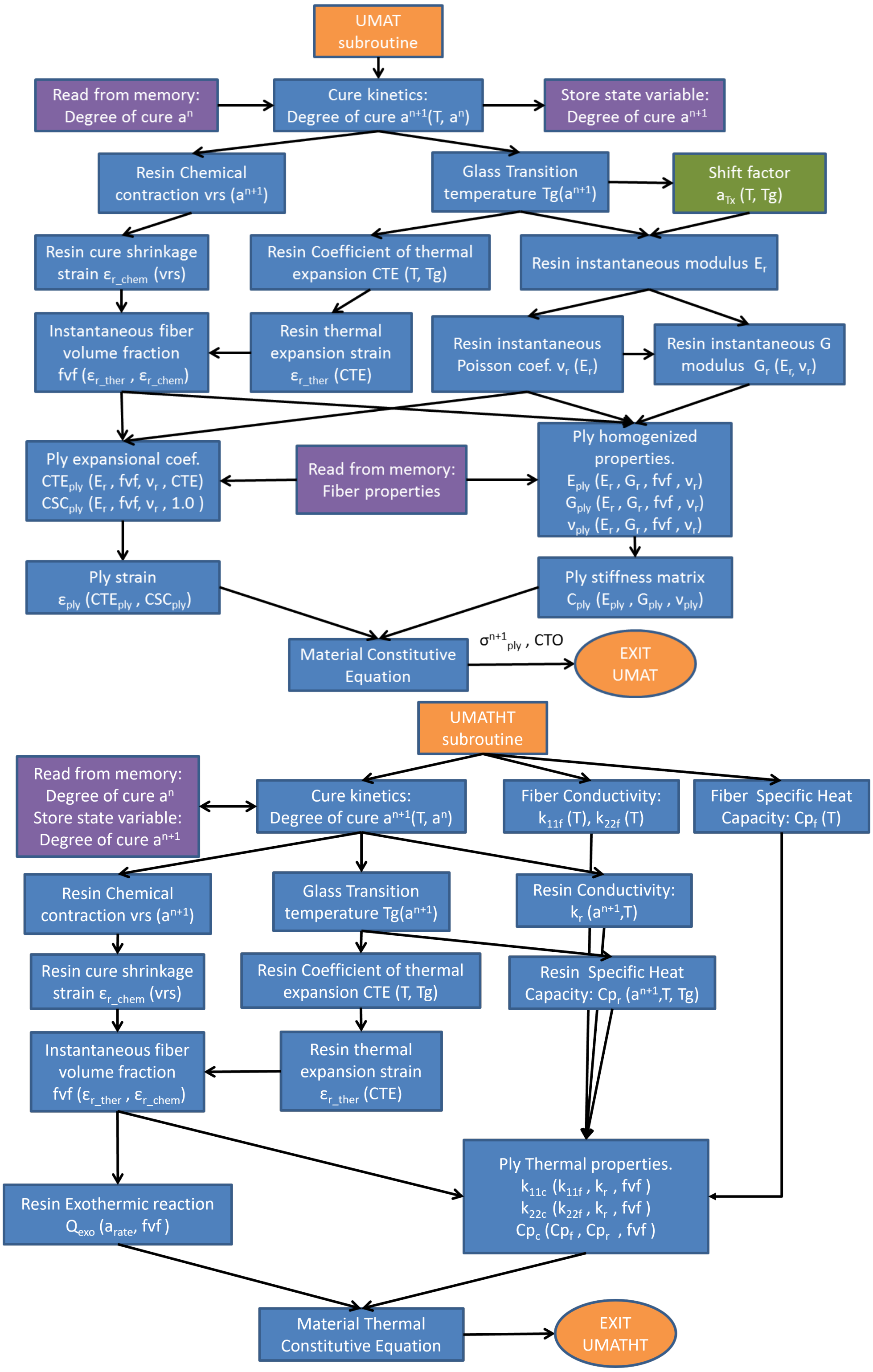

Figure 9: Diagram of the material modelling architecture (UMAT top used in the chemo-mechanical analysis, UMATHT bottom used in the thermal analysis.). Blue colour indicates variable calculation, purple access of memory, orange start/finish of the calculation process whereas the green box is employed only by the viscoelastic material model [70].

the INVAR tools, which are now used in the aerospace industry to manufacture structural parts because of their low Coefficient of Thermal Expansion (CTE) in accordance with the CTE of composite structures, with cheap alloys such as steel or aluminium. However, this requires experimental investigations for the material system and manufacturing process of interest, in order to determine the parameters of the friction model. Furthermore, the drawback of adding contact behaviour in the simulation process is that it increases the complexity of the simulation making it computationally demanding especially for large industrial parts.

In the context of the OptiMACS project, heat transfer analysis between the tool and the part was also investigated with the aim to identify significant temperature gradients across the part that could lead to property gradients in the part affecting its PID and dimensional stability. Thus, the already developed chemo-mechanical simulation approach was extended to a thermo-chemo-mechanical one. A subroutine (UMATHT) was developed in ABAQUS to take into account the exothermic heat reaction of the resin during cure and calculate the effective lamina thermal properties, namely the effective lamina conductivity and specific heat capacity as depicted in Fig. 9. With the use of this subroutine, the calculation of the temperature gradients across the part during the manufacturing cycle can be made. The challenge in the heat transfer analysis is to determine the heat transfer coefficient between the part and the tool which is a function of many variables (turbulence of the air in the oven, flow medium, pressure, temperature, etc.). In our case, two heat transfer coefficients were employed, one for the mould side and one to simulate the heat flow from the vacuum bag side of the part. The heat transfer coefficient values used in the simulation were supplied by Premium AEROTEC GmbH which measured the heat transfer coefficient in one of its ovens.

In the field of automation of the mirroring process for mould compensation the typical process would be to send to the design department the results of the first FE spring-in analysis in order to produce the updated mould surface. This surface is used usually for a second analysis in order to verify that the final product lies inside the predefined tolerance range before manufacturing the mould. In order to avoid the interaction between different departments which usually result in delays in the design process, three scripts were developed in the OptiMACS project to automate the mirroring process and produce the final mould surface, reducing the relevant design costs. One is used to mirror the 3D distortion field of the first spring-in analysis, the second one to translate and smooth the mesh of the untrimmed area (yellow as depicted in Fig. 10) to fit the trimmed element group (green as depicted in Fig. 10).This step is necessary because the trimming operation releases stresses and the subtraction of an element group from the model affects its distortion field. Finally, the last script is used to create CAD surfaces from the updated mesh geometry. Fig. 10 depicts the result of the application of the scripts in the mirroring process of the distortions of a U-section which is part of a composite frame (distortions multiplied by a factor of five for visualization purposes).

Finally, regarding the validation of the developed simulation framework, composite L-shape specimens were manufactured in the laboratory and measured with a Coordinate-Measuring Machine (CMM). Their spring-in angle was then compared with the simulation predictions of the two material models. Three moulds were manufactured from steel, INVAR

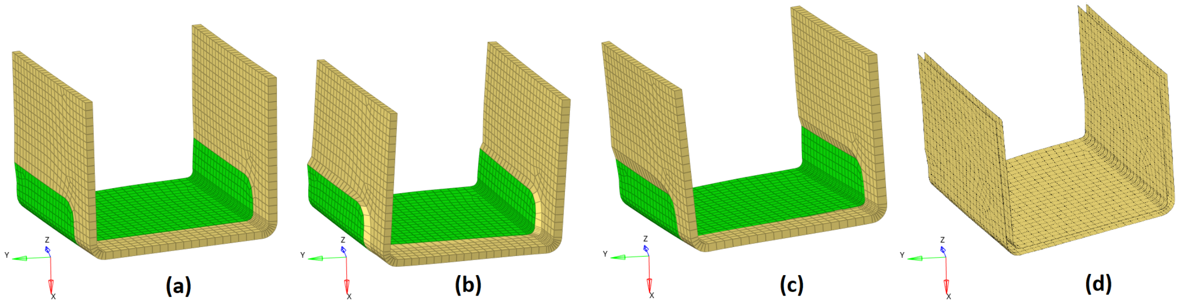

Figure 10: The steps employed to automate the mirroring process of the distortions of a spring-in analysis. a)Nominal geometry b)Result of the first spring-in analysis c) Mirroring of the distortions to the opposite direction c) Smoothing of mesh and creation of CAD surfaces (inner and outer).

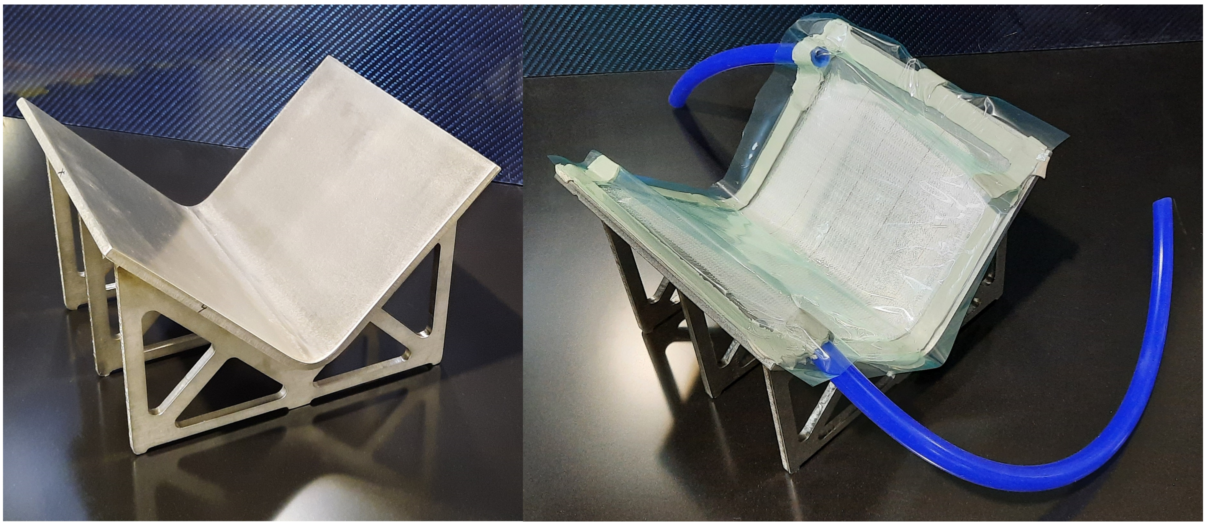

Figure 11: The steel L-shape mould used to manufacture the composite specimens before (left) and after the bagging process has been completed (right).

and aluminium alloys in order to monitor the effect of tool material on PID of the structures. Other factors that affect PID were also experimentally investigated such as specimen thickness and stacking sequence. Fig. 11 depicts one of the three moulds used to manufacture the L-shape composite specimens before and after the bagging process has been completed.

3.4. The global influence of local details

As discussed in Sec. 2.4, it is important to consider the design of some local areas during the design of the overall structure. The detail design of local areas is usually considered only after the global optimization has been performed. While this approach is not computationally expensive, it does not consider in full the effect of multiple local modifications on the design of the entire structure. Therefore, there is the possibility that a full global optimization will have to be performed again, which would result in costly delays.

As part of the OptiMACS project, a global-local MDO approach has been developed, in order to evaluate the influence of local design parameters and to check for local constraints violations already in the early stages of global design.

The optimization procedure is based on a monolithic architecture: the optimizer treats global and local design variables at once, thus considering the full design space.

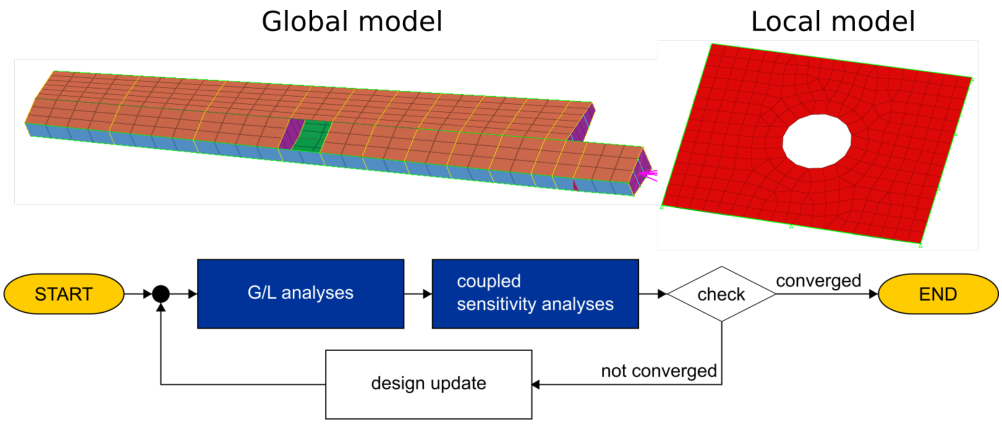

Figure 12: Global-local monolithic MDO flowchart.

As depicted in Fig. 12, in each optimization iteration all disciplines are solved and the sensitivities are computed, by adopting a global-local approach. In particular, two different types of analysis have been considered: linear static analysis and linear static aeroelastic analysis.

The global-local analysis strategy is based on three operations performed in sequence: Guyan condensation of the local information [81], solution of the global model with the condensed local information, solution of the local models. In the first step, stiffness matrix and load vector of the local models are reduced with respect to the DOFs interfaced with the global model. This results in a reduced stiffness matrix and a reduced load vector containing respectively stiffness and load contributions related to the boundary DOFs shared by the global and the local models. Next, the entries of these reduced quantities are added to the stiffness matrix and load vector of the global model. With the added local information, the resulting solutions of the global analyses are affected in such a way as to take into account the influence of the local models. In particular, in the case of static analysis and static aeroelasticity, the solutions are the same that would be obtained, if a unique model with the same mesh, obtained by joining global and local models, was solved. In the last step, the local models are separately solved by using the computed global solution as a Dirichlet boundary condition, applied at the interface between global and local models.

Once the analyses are completed, a coupled sensitivity analysis is performed. This global-local sensitivity analysis takes into account global and local constraints and global and local design variables. Thus, it captures the interaction between global and local design choices or, more precisely, the influence of global design variables on local constraints and the influence of local design variables on global constraints. This essentially means to capture the influence of the design variables of one model on the solution of another one. And since the solutions are computed following a special global-local analysis strategy, the global-local sensitivity analysis requires an ad-hoc formulation.

Thanks to the fact that the sensitivity analysis considers local constraints and design variables as well, the optimizer can then take advantage of the additional freedom provided by the local design space, while at the same time ensuring the feasibility of the local design. Furthermore, by computing the sensitivities of active constraints only, the impact on the overall computational cost is limited.

3.5. Seamless integration of software tools

As indicated in Sec. 2.5, there is a need to improve the integration of the software packages used in the design evaluation process by automating data generation and transfer between these packages. In the work carried out during the OptiMACS project, implementation of this automation has been focused on the structural interface between wings and fuselage. Several bottlenecks in the data transfer process have been identified and addressed in this work, such as i) definition of structural interfaces; ii) definition of wing cut-out; iii) automated assignment of sizing variables and constraints; iv) automated processing for flight conditions and load cases; and v) automated generation of aero-structural coupling input. The structural interfaces are categorised as discrete and continuous [120], where for the discrete structural interface, attributes are defined for joint position, stiffness, material properties and thickness of the joint elements. For the continuous structural interface, references for the connecting structures are created as well as a reinforcement structure such as a cruciform, triform or buttstrap. Furthermore, a new cut out element, defined by ribs, spars, and/or relative coordinates, has been created and used to define a patch on one side of the wing skin with different material properties or stringer definition. Moreover, a method for automatic assignment of sizing variables based on information recorded from choices made by engineers has been developed and implemented as a Python program. Similarly, a tool for automated reading of the the information from the design file and conversion of the parameters required by the optimizer has been implemented. Finally, to allow for coupling between the structural and aerodynamic model, the tool for automatic generation of coupling input has also been developed.

The developed interfaces, highlighted in blue boxes in Fig. 13, have resulted in a streamlined process giving a significant reduction of the time taken from an average of two months to approximately an hour (for a large airframe design with over 10^5 DOF, about 8×10^4 sizing variables and 2×10^5 constraints in the FEM structural model). A large proportion of the time needed for current automated evaluation is attributed to the sizing optimization in *Lagrange*, followed by the generation of the structural model. With this automation, it greatly improves the overall efficiency for airframe design evaluation and opens up the possibility of MDO for the airframe design.

4. OptiMACS contributions to the efficient and optimal design of airframe structures — case studies

4.1. More efficient stacking sequence optimization for aircraft structures

The two-stage optimization process presented in 3.1 has been applied to the wing covers of OptiMALE, an industrial-scale demonstrator shown in Fig. 2. The aircraft is modelled

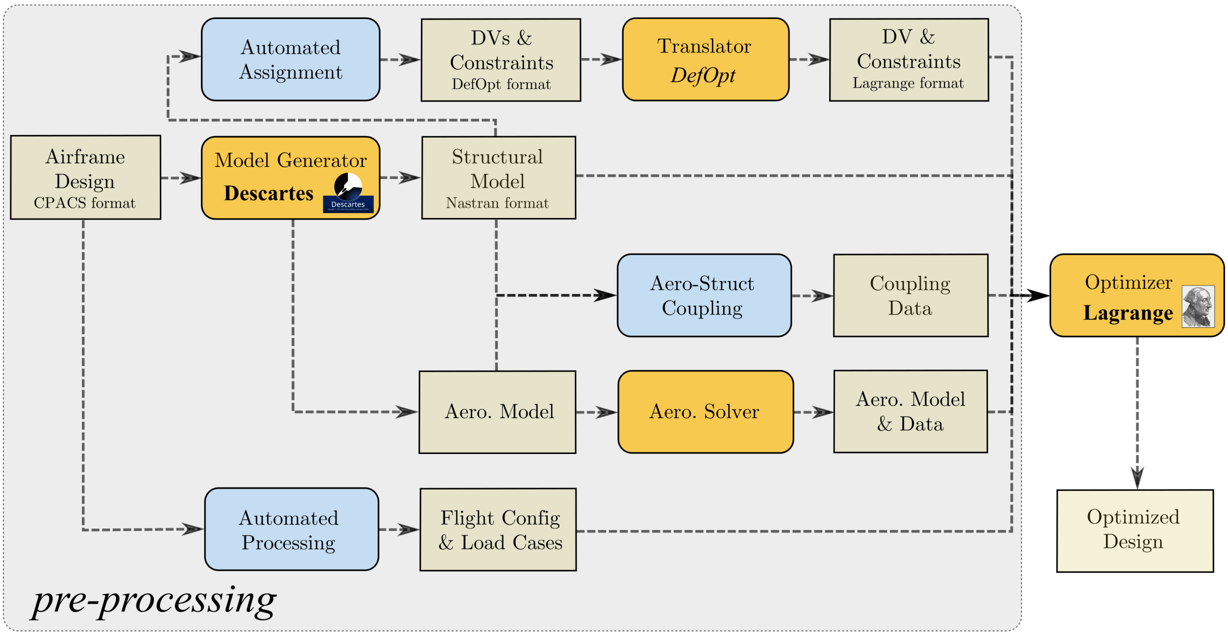

Figure 13: The improved workflow of an airframe design performance evaluation.

using a coarse Global FE model (GFEM) consisting of 1D and 2D structural elements. The model is subjected to 19 static load cases which have been preselected from a complete flight envelope covering different operating altitudes, Mach numbers and load factors. In this work, only the wing of the aircraft is studied and therefore the wing skins, spars, stringers and ribs are represented using a total of approximately 3000 design variables. Besides strength and buckling constraints, manufacturing constraints are also applied to the skin of the wing. More specifically, blending and maximum ply drop constraints are applied between neighbouring laminates. This leads to a total of more than 570,000 constraints.

The outer part of the wing of the aircraft is detachable due to storage requirements which leads to a total of 4 sub-components, 2 for each of the upper and lower parts of the wing skin. The patches on the upper and lower skin of the wing which can be seen in Figs. 14a and 14b have been chosen manually, using more, smaller patches towards the root of the wing where the thickness gradients are expected to be steeper. A total of 134 patches have been used in this study. Concerning the number of generic layers used to model the stiffness properties of the structure, a maximum of 32 generic layers resulting in 12 design variables due to symmetry and balance requirements have been used for the thickest regions of the wing covers. For the thinnest, outer parts of the wing, 8 generic layers leading to 3 design variables for each patch have been chosen to model the properties of the structure. Modelling each patch with an appropriate number of generic layers depending on the expected thickness is of high importance, because an inadequate generic stack can lead to an erroneous continuous stiffness outcome, which in turn cannot be matched during the discrete optimization stage resulting to violation of physical constraints in the structure. For example, using significantly more generic layers than the actual thickness of the patch, offers a large design freedom which cannot be matched in the discrete stage. On the other hand, when two neighbouring patches are modelled with a different number of generic layers, the blending constraint cannot be formulated precisely on a layer to layer basis but is rather inexactly applied to the total number of layers per orientation [85]. This can in turn also lead to continuous results that cannot be precisely matched in the second stage. Therefore, the number of neighbouring patch interfaces where a different generic stack is used must also be kept to a minimum. The gradient-based optimization converges to a continuous thickness distribution of the skins of the wing which results to a mass of 226.8 kg.

The total, continuous thickness of each patch is rounded up to an integer number of discrete layers, while maintaining the number of each individual fibre orientation $[0, 90, \pm 45]$ above a safety threshold to assist with the satisfaction of strength constraints in the discretized structure. The discrete optimization is performed using the decomposition technique mentioned in Sec. 3.1. Small physical constraint violations were observed after evaluating the discretized solution with *Lagrange*. For the skins of the wing, the minimum Reserve Factor (RF) observed for strength was 0.99. The RF is the ratio of the allowable over the applicable load, so a $RF < 1$ indicates a constraint violation. Slightly bigger violations were observed for the buckling constraints of the spar webs and stringers, namely a minimum RF of 0.93 and 0.90 respectively. These components were not discretized and the reason for the constraint violations is load redistribution due to the discretization of the wing skin laminates which attracted more loads in some areas. One solution to the constraint violations of the discretized structure is to increase the design factor on the Finite Element Model and perform the two stages of the optimization again. However, this process is time consuming and would also end up increasing the weight of the structure quite significantly due to multiple components of the wing being unnecessarily overdimensioned. Instead, since only very minor constraint violations were observed for the wing skins which were the parts of the structure to be discretized, the first stage of the optimization was performed again while keeping these discrete laminates constant during the optimization. Instead, the design variables for the spar webs and stringers, which were not discretized, were all active. This led to the fulfilment of all structural constraints on the wing for both the spar webs and stringers, but also the wing skins. The mass penalty during this corrective process was only 3 kg with the discretized wing skin being 235.1 kg showing only a 3.7% increase compared to the original continuous result.

Even though the contributions of the work performed on the stacking sequence optimization towards the overall detailed sizing capabilities of *Lagrange* cannot be explicitly quantified, they can be divided in two categories. First of all, the introduction of the second stage of the optimization automates the retrieval of good quality solutions satisfying a wide range of guidelines. Since this task used to involve a lot of manual effort and re-iterations, the sizing process has become more time efficient. Secondly, the introduction of composite constraints in the first stage of the optimization, bridges the information gap between the two optimization stages leading to minor constraint violations after the discretization of the structure which would otherwise need to be resolved by introducing large design factors. Besides forcing the entire two-stage process to be repeated again, these design factors would also lead to over-dimensioning of entire components, leading to a significantly higher mass penalisation.

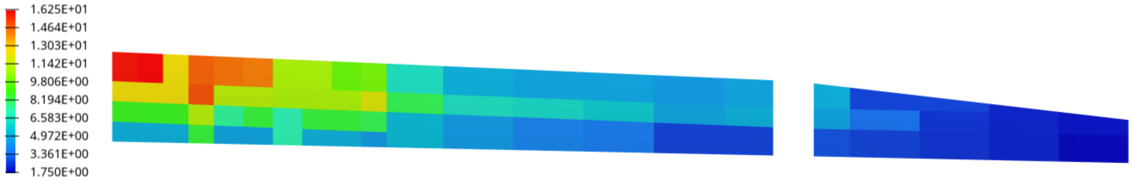

(a) Thickness distribution for the upper wing cover.

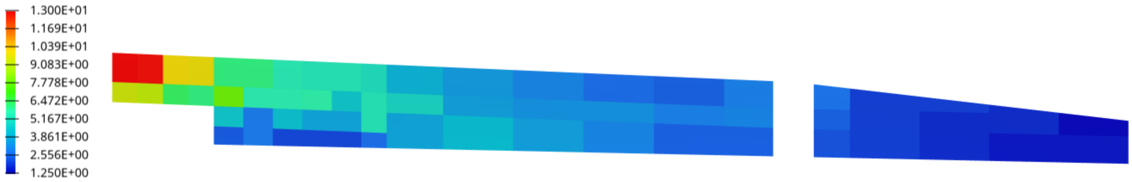

(b) Thickness distribution for the lower wing cover.

Figure 14: Thickness distribution for the final, discrete laminates of the OptiMALE demonstrator aircraft.

4.2. Integration of detailed failure models within the MDO for accurate and efficient damage-resilient aircraft design

This section presents examples of application of the failure methods introduced in Sec. 3.2. In the next subsection, extended omni strain failure envelopes are correlated with experimental data from the literature in order to validate their predictions for composite laminates. Then, the following subsection presents a case study of the "hot spot" identification method.

4.2.1. Validation of extended omni strain failure theory

The failure theory outlined in Sec. 3.2.1 was developed to generate fast and safe predictions of failure for FRP laminates. Herein, to assess the performance of this failure theory, extended omni strain failure envelopes are tested against experimental evidence. Furthermore, the obtained failure envelopes are compared with the omni strain failure envelope based on Tsai-Wu failure theory, to study the strengths and limitations of the proposed extension.

In particular, a validation study of the predicting capability of the extended omni strain failure concept was performed using experimental results from the first and second World-Wide Failure Exercise (WWFE) [121, 122]. Firstly, several test cases from the WWFE-I, involving multidirectional laminates under biaxial loads, were selected. Among these test cases, two are shown in Fig. 15, where omni FPF/LPF envelopes, obtained using the 3D invariant-based failure theory and Tsai-Wu, are correlated against experimental data for a AS4/3501-6 [90/±45/0]s laminate (Fig. 15a) and a E-glass/LY556/HT907/DY063 [±30/90]s laminate (Fig. 15b).

An excellent agreement can be observed for the 2D test data when considering omni LPF envelopes, except for the compression-compression quadrant where the predictions overestimate the laminate strength under biaxial compression. These less accurate predictions are justified by a reported buckling occurred in those specimens, leading to a premature failure in both laminates [122]. The biaxial test cases provide also a clear indication on the huge benefits in using a LPF approach instead of FPF predictions. The larger domain when using LPF predictions allows to reduce conservatism in a remarkable way, without incurring additional computational time. These benefits can be exploited immediately from the conceptual design stage of composite aerostructures, since the presented tool is invariant with respect to the laminate layup. The beneficial impact of this approach on the composites industry, where the consolidated practice in early design stage is to use FPF theories, such as maximum strain or Tsai-Wu criteria, can be significant.

It can be noted that a good correlation with these experimental data was already achieved by competing failure theories involved in the WWFE (such as the criteria developed by Puck and Schürmann) [122]. However, the unique feature of the omni strain failure concept (for both theories) is that laminate failure predictions require only the material properties extracted from the UD material. Despite the two omni strain failure envelopes provide similar failure prediction for biaxial test cases, the added value brought by the proposed envelopes can be still highlighted when analysing glass-fibre composites, whose LPF is governed by different failure modes (as shown in [94]); LPF of CFRP laminates, on the other hand, is always governed by fibre failure, as confirmed by this analysis.

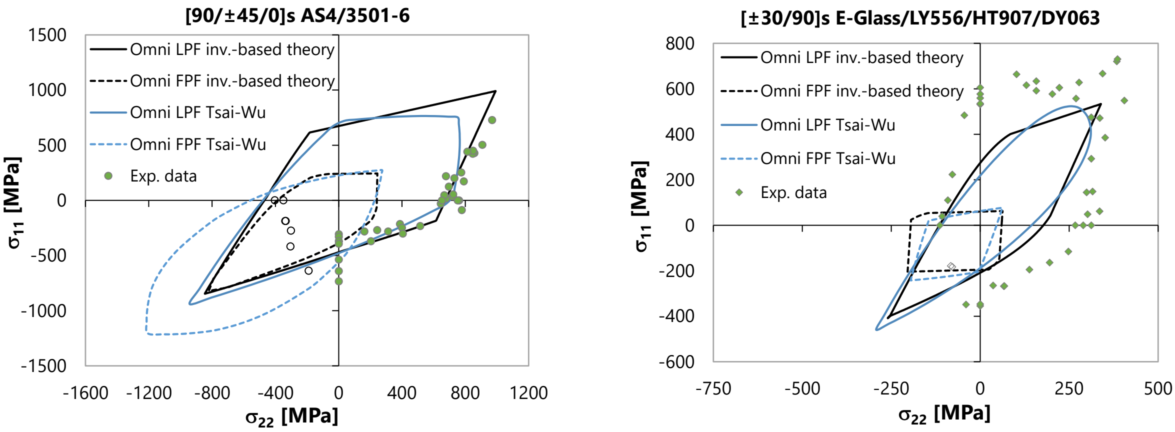

(a) [90/±45/0]s AS4/3501-6 carbon/epoxy.

(b) [±30/90]s E-glass/LY556/HT907/DY063.

Figure 15: Omni FPF/LPF envelopes versus experimental results from WWFE-I for a [±30/90]s E-glass/LY556/HT907/DY063 laminate and a [90/±45/0]s AS4/3501-6 carbon/epoxy laminate.

Then, a triaxial test case for laminate failure from the WWFE-II was considered. The few available experimental results show the evolution of the transverse compressive strength σ_{22} with through-thickness stress σ_{33} (where $\sigma_{11}{=}\sigma_{33}$) of a glass/epoxy angle-ply laminate (±35°). Using the mechanical properties of E-glass/MY750/HY750/DY063 in the out-of-plane direction from [123], a 3D omni LPF surface was generated and correlated with the failure loci. Additionally, to assess the conservatism of the proposed 3D omni LPF surface, a laminate LPF surface obtained superposing only ply failure surfaces of the relevant orientations (±35°) and the same failure model, was included in this study. The correlation of these surfaces with experimental data, presented in Fig. 16, shows that the laminate LPF envelope allows to reduce the conservatism of 3D omni LPF surfaces in the case of angle-ply laminates. However, the omni LPF envelopes define, in a physically-based setting, a safe approach for laminate failure prediction that is independent of the particular stacking sequence, thus can be applied to any laminate of a given material system. This can be better assessed in Fig. 17, where the relevant sections of these failure surfaces are compared with experimental data. In this figure, the omni strain LPF envelope based on Tsai-Wu failure theory are also included, showing that the design space is considerably reduced in the first and third quadrant, as a result of the effect of the out-of-plane stress, accounted in the omni LPF surfaces. This means that the influence of the out-of-plane stress cannot be neglected to properly capture laminate failure under hydrostatic pressure and to obtain safe LPF predictions under general 3D stress states.

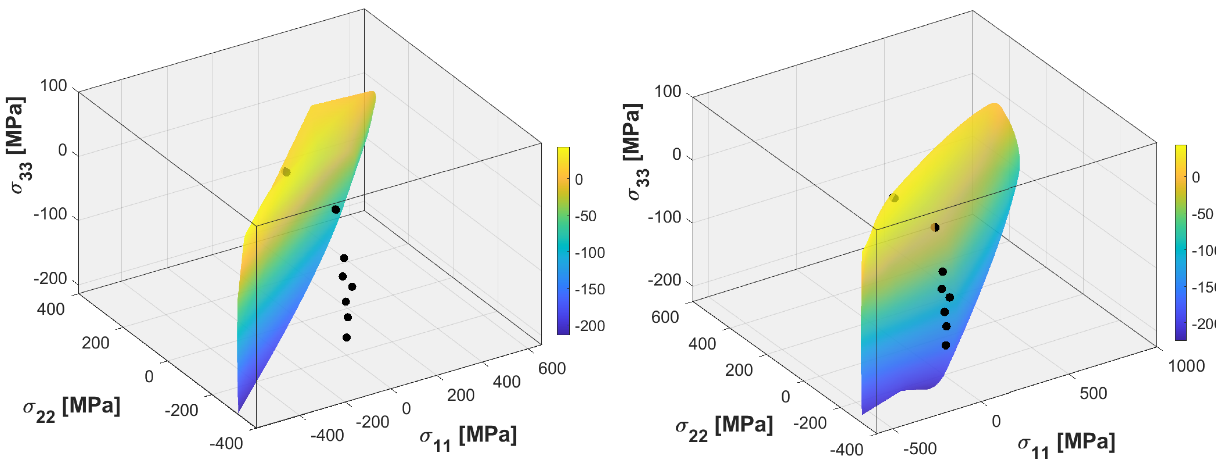

(a) 3D omni LPF surface.

(b) 3D [±35]s LPF surface.

Figure 16: 3D omni LPF (a) and [±35]s laminate LPF (b) surfaces versus experimental results from WWFE-II for a [±35]s E-glass/MY750 epoxy laminate.

4.2.2. Example of application of the detailed failure model

An example of application of the “hot spot” identification method, as described in Sec. 3.2.2, is shown in Fig. 18. In this case, the hot-spot failure analysis is applied to an aeronautical reinforced panel, targeting the identification of the critical locations for damage onset in the runout region. For the discretization of the structure under analysis, first-order solid elements are preferred over shell elements, because only the first ones can account for components of the full set of the stress tensor, playing a crucial role in the runout region, where a change of load path takes place.

Since the results show that the onset of damage in the skin region close to the runout is triggered by fibre kinking, a detailed model of that area was built to perform local failure analysis and study the fibre kinking onset and broadening. In this way, the evolution of damage due to fibre kinking can be studied up to collapse. However, in general, a material

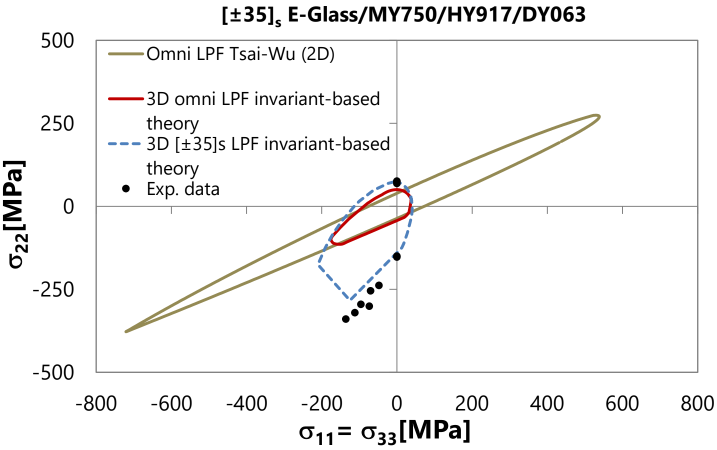

Figure 17: Correlation of 3D omni LPF, 3D laminate LPF and omni LPF based on Tsai-Wu with experimental data from WWFE-II for a [±35]s E-glass/MY750 epoxy laminate.

model representing the initiation and propagation of all failure modes can be also implemented. In this way, the mechanical response of the reinforced panel up to final collapse can be predicted more accurately, but a full model involves higher computational costs.

Additionally, in those areas where delamination or debonding is predicted to take place, cohesive elements can be introduced in the FE-model to accurately predict the onset and propagation of these phenomena. As an example, in Fig. 19, the delamination growth in a open-hole laminate is shown by highlighting the cohesive elements with different colours: in green the ones partially damaged (with a damage variable between 0.10 and 0.99), in blue the ones where damage is in its early stage (with a damage variable between 0.001 and 0.10) and in red the ones severely damaged (with a damage variable greater than 0.99). The elements that are not damaged take an initial colour which has been set as white. The damage variable of the cohesive elements is calculated from the evolution law implemented in Abaqus and proposed in [124].

As a remark, OptiMACS research on failure models allowed mainly to deliver two novel contributions: i) the development of a fast tool to predict laminate LPF under general 3D stress states through the concept of omni LPF envelopes and ii) an extended composite material model to account for the effect of out-of-plane stress components in the initiation and broadening of fiber kinking.

4.3. Manufacturing distortions

The CHILE and the viscoelastic material models presented in 3.3 were applied to predict PID of L-shape composite structures. A thermo-chemo-mechanical simulation approach was employed in this case and tool part interaction was also investigated regarding its effect on simulation results. By performing an extensive numerical investigation on these structures it was found that the fixed boundary condition produces the minimum distortion (spring-in angle), whereas the free-standing boundary conditions the maximum expected distortions (spring-in angle). The tool part interaction predictions lie in between the values predicted

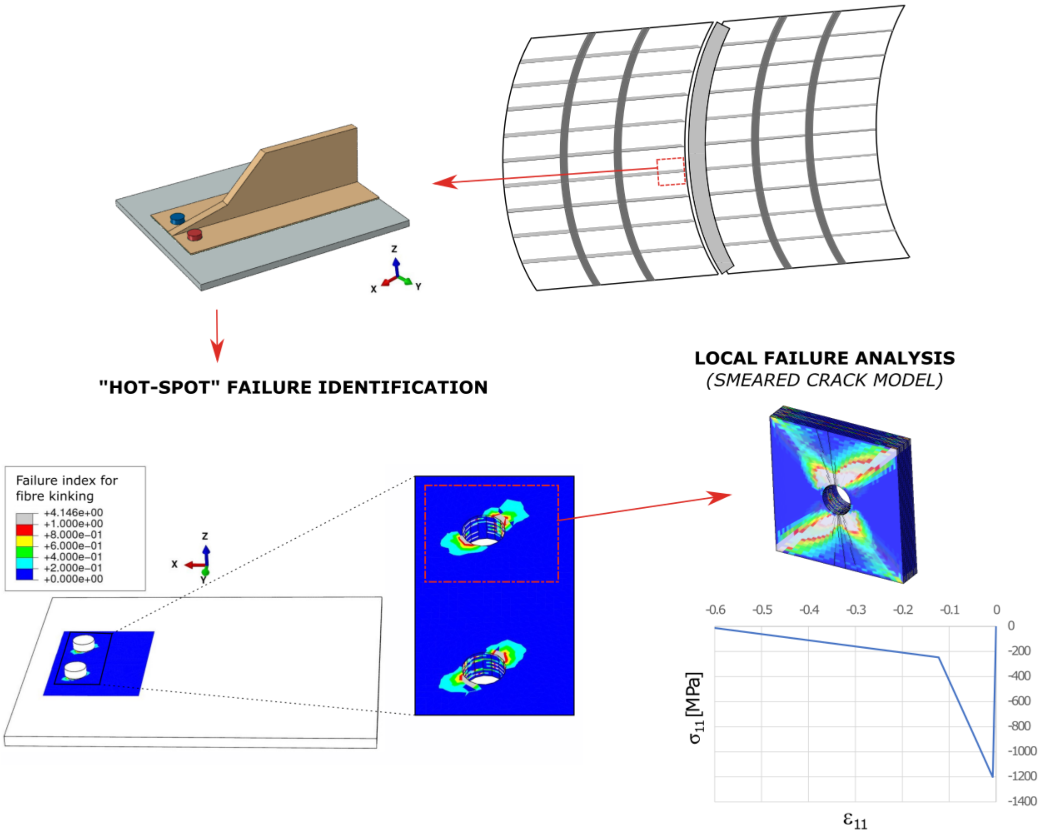

Figure 18: Illustration of the local analysis strategy to capture failure with detailed damage models.

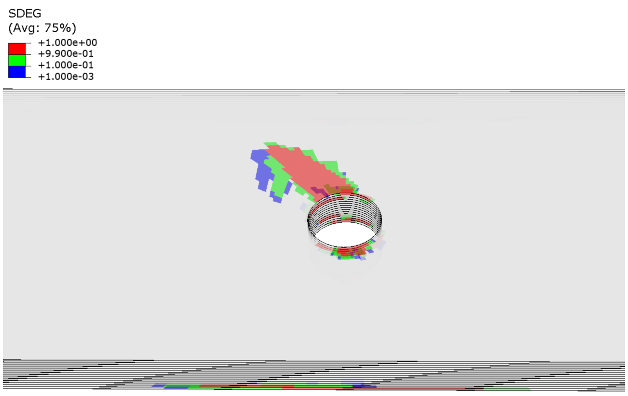

Figure 19: Prediction of delamination growth for a quasi-isotropic open-hole laminate, by using a damage variable for cohesive elements (transparency level: 50%).

by the fixed and free-standing boundary conditions for most of the cases studied. Fig. 20 depicts a comparison of the distortion predicted by employing different boundary conditions for the case of an L-shape structure having a stacking sequence representative of an aerospace frame.

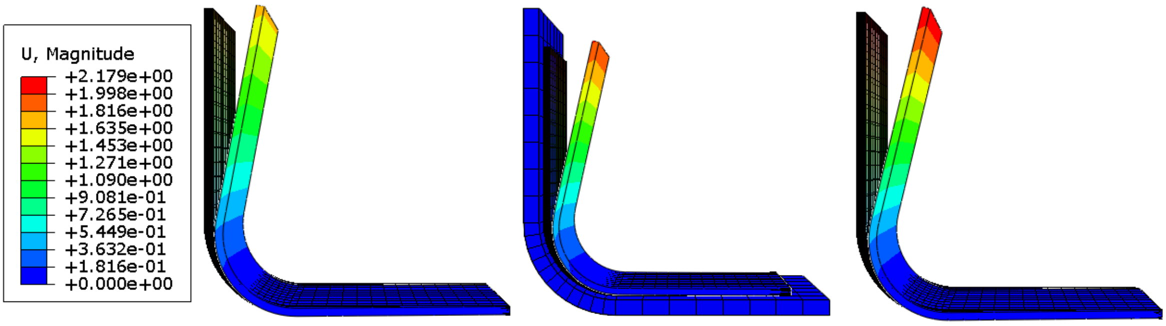

Figure 20: Distortions in mm of a L-shape composite structure at the end of the curing cycle using the CHILE material model with the use of fixed (left), tool-part interaction (middle) and free-standing (right) boundary conditions.

The CHILE and the viscoelastic material models were also applied to predict PID of an aerospace test frame of industrial size (Fig. 21). Even if this frame is only intended for research purposes, it has many common features with flying frames used in aircraft fuselages as the one depicted in Fig. 2 for the case of OptiMALE. To simplify the analysis, in this case study a chemo-mechanical simulation approach was adopted by assuming a homogeneous temperature field across the part at every time step, which is a product of manufacturing experience.

By comparing the predictions of the two material modes with the 3D scanned shape of the frame, it was found that the viscoelastic material model could predict more accurately the shape distortion of the part compared to the CHILE material model which was found to overestimate in magnitude the distortion of the frame [70, 125]. Consequently, in the context of the OptiMACS project, viscoelastic material models are proposed to predict shape distortions of aerospace thermoset composite parts when the maximum prediction accuracy is sought. However, taken into account the increased material characterization effort and cost needed by viscoelastic material models to run, along with their increased calculation time due to the calculation and storage in memory of state variables, the CHILE material model is regarded to be a good compromise between cost and performance.

Regardless of the material model chosen to predict PID of the frame (CHILE or viscoelastic), the use of the simulation framework developed in OptiMACS (Fig. 9), enabled the prediction of a complex distortion field (Fig. 21). This could not be predicted by simple analytical equations or manufacturing experience, usually employed in the shop floor.

Finally, Fig. 22 depicts a tool part interaction simulation that was performed by employing an aluminium mould and a cure dependent CoF of a U-shape composite structure. It was found that the aluminium mould compresses the composite part at the end of the cool down phase (end of curing cycle) due to the great difference of CTE of the aluminium and composite structure, showing that tool part interaction plays an important role in this application.

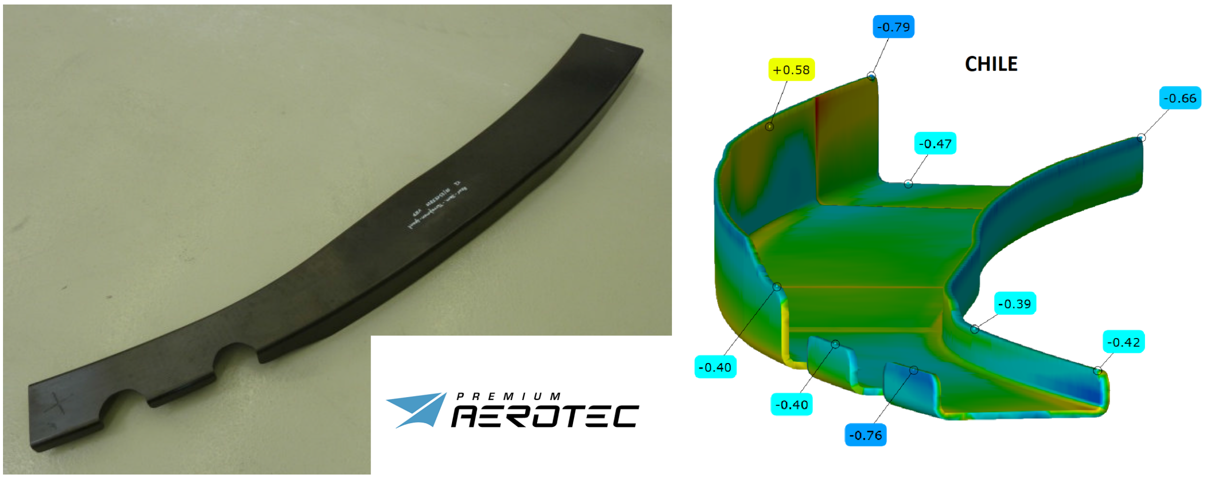

Figure 21: Industrial test frame (left). The expected distortions of the frame with the use of the CHILE material model (right).

4.4. Global-local MDO

The procedure for global-local MDO presented in Sec. 3.4 can be applied to the weight minimization of a model like the wingbox represented in Fig. 23.

The rectangular area highlighted in red represents a local structure modelled in a separate FE-model. The entire structure is optimized by modifying 159 design variables, representing the thicknesses of shell elements and cross sectional area of bar elements. Of these 159 design variables, one is used to design the local model while instead 158 parametrize the global model. Strength constraints are applied to both the global and the local model. By applying the monolithic approach presented in Sec. 3.4, it is possible to obtain the optimized thickness distribution of the structure, while satisfying both global and local constraints.

Fig. 24 shows a comparison between a reference thickness distribution and the global-local optimal thickness distribution obtained for the same static analysis subcase. Fig. 24a shows the optimal thickness distribution obtained without the application of a global-local strategy and using a single coarse model, which does not capture in detail the local geometry. Using a separate refined local model and the global-local strategy presented in Sec. 3.4, the obtained optimal thickness distribution is the one shown in Fig. 24b.

Analogously, Fig. 25 shows the same comparison for an aeroelastic analysis subcase.

The global-local analysis of each subcase is solved by condensing the local model, solving the global model by adding the local contributions and solving the local one with the global solution as a boundary condition. The sensitivities are computed with the global-local methodology described in Sec. 3.4.

In both cases, the obtained thickness distributions are different and, in particular, the optimal local model design is thicker in order to satisfy the local constraints, while accommodating the cut-out.

The reference approach was based on a fixed and unconstrained coarse representation of the local geometry, in order to contain the computational cost of the procedure, and was not guaranteed to yield a locally feasible final design. In contrast, the presented global-local

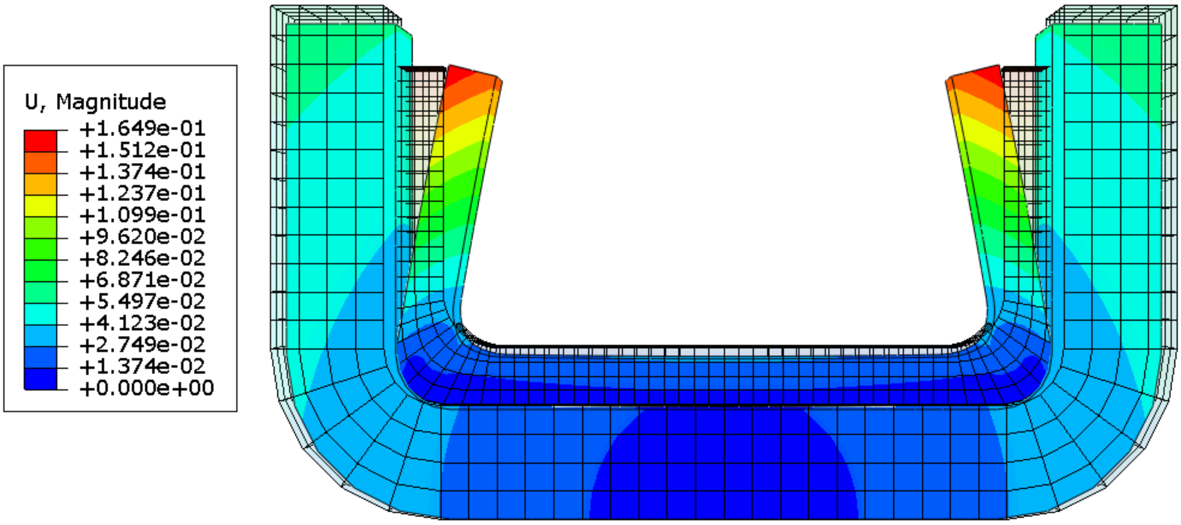

Figure 22: Distortions of a U-shape composite structure at the end of the curing cycle using the CHILE material model (cm).

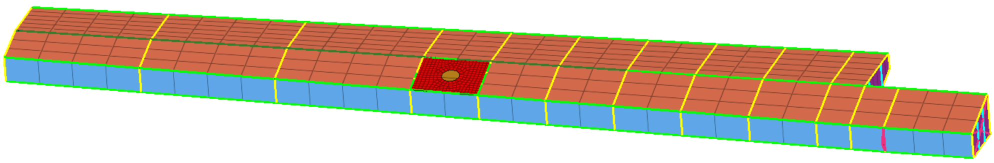

Figure 23: Global-local modelling of a wingbox.

approach effectively minimizes the structural weight, while ensuring that all constraints are not violated, including those defined over the locally refined model. Thus, the approach effectively minimizes the chance that an update of global design will be needed.

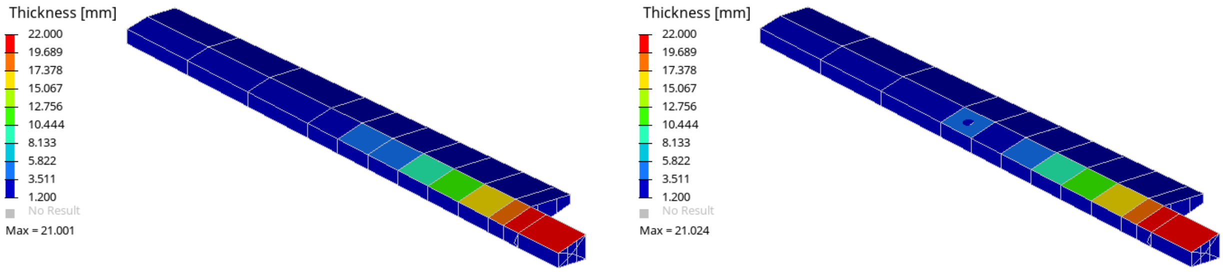

(a) Reference thickness distribution.

(b) Global-local optimal thickness distribution.

Figure 24: Comparison of optimal thickness distributions for a static analysis subcase: without (left) and with (right) application of local refinement and global-local strategy.

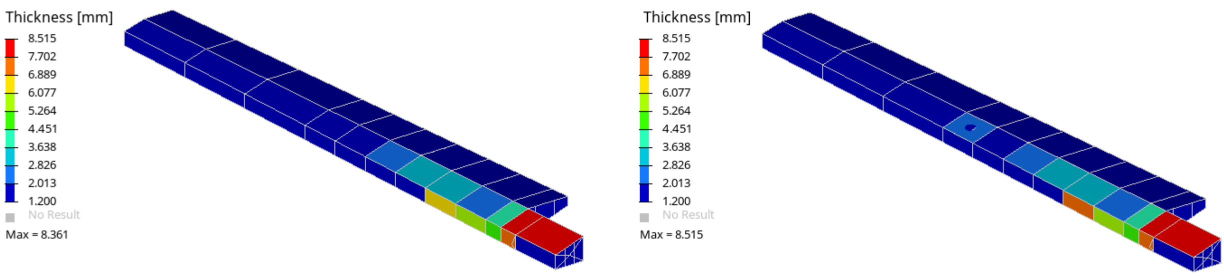

(a) Reference thickness distribution.

(b) Global-local optimal thickness distribution.

Figure 25: Comparison of optimal thickness distributions for an aeroelastic analysis subcase: without (left) and with (right) application of local refinement and global-local strategy.

5. Concluding remarks and anticipated future developments

Some of the major industrial challenges to achieve optimal structural designs are hereby discussed. The need for accurately capturing the performance characteristics of each design candidate early in the preliminary, or even in the conceptual stage has provided motivation and impulse towards new MDO technologies. Emphasis is particularly given on the opportunities and challenges arising through the employment of composite materials. Recent developments in the aeronautical sector are globally oriented towards capturing more detail of the structural product within the MDO loop at minimum or no additional computational cost.

In this manuscript we discuss the challenges and potential impact of the following specific structural disciplines which are under intense development within the modern aeronautical industry. The contribution of the OptiMACS project towards these contemporary challenges is also exhibited with concrete case studies also provided.

- The optimal design of large laminated structures with intense thickness variations over their surface is associated with a number of challenges due to the mixed discrete and continuous nature of the problem. Hence, in the place of a traditional design development process, two-stage optimization approaches are becoming more popular within the aeronautical sector. Such approaches are hereby discussed. It is demonstrated that a two-stage optimization process has the potential to lead to solutions satisfying all required structural constraints for a lower component mass.

- Accounting for structural resilience against damage accumulation early in the design process is another major challenge for the next generation of MDO processes. Inclusion of more accurate failure criteria is expected to enable lighter designs through relaxation of safety factors as well as inclusion of phenomena such as reversible local buckling. The manuscript discusses the application challenges and development of global-local failure methodologies. As a case-study representative for the aeronautical sector, extended omni-strain failure envelopes are correlated with experimental data from the literature in order to validate their predictions for composite multi-directional laminates, while the hot-spot failure identification method is employed to predict the most critical areas and failure modes in a reinforced panel, addressing then the critical regions with detailed damage models.

- Addressing the presence of process induced distortions is another major challenge when composite materials are to be implemented in the design. This is mainly due to their peculiarities related to resin chemical shrinkage, tool part interaction, temperature gradients and stress relaxation amongst other factors. The computational challenge of considering these manufacturing parameters in the design process of moulds, having a optimized shape, in order to achieve a "First Time Right" approach in the manufacturing of composite structures, was also discussed in the manuscript.

- The integration of local structural complexities within the MDO procedure generally comes with added computational burden. It is however critical for accounting the impact of such complexities on the airframe design and avoiding an extremely conservative, sub-optimal design due to lack of this local information. In this manuscript a global-local analysis strategy is discussed, based on Guyan condensation of the local information and subsequent solution of the global and local models. A global-local sensitivity analysis, combined with an active set optimization strategy, allows to account for local constraint violations at an acceptable computational cost.

- The seamless integration of software tools is another major challenge especially when an integrated multiscale framework is to be implemented able to exchange information between the preliminary and conceptual design stages. We hereby discussed challenges related to structural interface definitions, assignment of sizing variables and constraints, automated processing for flight conditions and load cases, as well as automation of the aero-structural coupling.

Future work in the aeronautical MDO sector is expected to rely on an increased level of detail during preliminary sizing of a structural model and complete quantitative evaluation of its performance with a limited computational cost. For instance, research is currently working to account for inspectability and manufacturability aspects in the MDO process, which is found to play a crucial role in the lifecycle of an aircraft. Pushing MDO within the conceptual design stage will be challenging for structural engineers over the next few years; it is however certainly the global vision over decades to come. Such an advancement will effectively *erase any solid boundaries between the conceptual and preliminary stages, eventually unifying the design optimization process.* Multidisciplinary developments in the fronts of more efficient physics models, metamodelling (efficient surrogate predictions in order to radically reduce design evaluation times), parallel computing and FE model reduction schemes are all very welcome in order to synergistically achieve the above vision.

6. Acknowledgements

This work was supported by the H2020 Marie Sklodowska-Curie European Industrial Doctorate OptiMACS (Grant 764650). José Reinoso has received funding from the Clean Sky 2 Joint Undertaking under the European Union's Horizon 2020 research and innovation programme under grant agreement No. 785463.

List of abbreviations

ATL Automatic Tape Laying

CFRP Carbon Fibre Reinforced Plastics

CHILE Cure Hardening Instantaneous Linear Elastic

CMM Coordinate-Measuring Machine

CoF Coefficient of Friction

CPACS Common Parametric Aircraft Configuration Schema

CTE Coefficient of Thermal Expansion

DLR Deutsches Zentrum für Luft- und Raumfahrt - German Aerospace Center

DOF Degree Of Freedom

FE Finite Element

FEM Finite Element Method

FPF First-ply failure

FRP Fibre-reinforced polymer

GFEM Global FE model

GUI Graphical user interface

LPF Last-ply failure

MDO Multidisciplinary Design Optimization

MILP Mixed Integer Linear Programming

NCF Non-Crimp Fabric

OptiMACS Optimization of Multifunctional Aerospace Composite Structures

PID Process Induced Distortions

RBDO Reliability-Based Design Optimization

RDO Robust Design Optimization

RF Reserve Factor

TIGL TIVA Geometric Library

TIVA Technology Integration for the Virtual Aircraft

UD Unidirectional

XML eXtensible Markup Language

XSD XML Schema Definition

WWFE World-Wide Failure Exercise

References

1. Ullman, D.G.. The mechanical design process. McGraw-Hill series in mechanical engineering; 4th ed ed.; Boston: McGraw-Hill Higher Education; 2010. ISBN 978-0-07-297574-1 978-0-07-126796-0. OCLC: ocn244060468.
2. Elssel, K., Petersson, Ö.. CA-AeroStruct - Multidisziplinäre Optimierung und Simulation zukünftiger Hochleistungsplattformen Schlussbericht. A ed.; Manching: Airbus Defence and Space GmbH; 2016. URL: `https://edocs.tib.eu/files/e01fb16/869934570.pdf`.
3. Arora, J., Wang, Q.. Review of formulations for structural and mechanical system optimization. *Structural and Multidisciplinary Optimization* 2005;30(4):251–272. URL: `https://www.scopus.com/inward/record.uri?eid=2-s2.0-24944454675&doi=10.1007%2fs00158-004-0509-6&partnerID=40&md5=0f258a91bfea85b0382c9986c7c0768e`.
4. Wang, C., Zhao, Z., Zhou, M., Sigmund, O., Zhang, X.. A comprehensive review of educational articles on structural and multidisciplinary optimization. *Structural and Multidisciplinary Optimization* 2021;64(5):2827–2880. URL: `https://www.scopus.com/inward/record.uri?eid=2-s2.0-85116317755&doi=10.1007%2fs00158-021-03050-7&partnerID=40&md5=250e4882488813129ca7f99146796fa7`.
5. Fredricson, H.. Structural topology optimisation: An application review. *International Journal of Vehicle Design* 2005;37(1):67–80. URL: `https://www.scopus.com/inward/record.uri?eid=2-s2.0-14844297422&doi=10.1504%2fIJVD.2005.006089&partnerID=40&md5=92f41b68be7bb8fbb97ed1e7025b22d5`.
6. Deaton, J., Grandhi, R.. A survey of structural and multidisciplinary continuum topology optimization: Post 2000. *Structural and Multidisciplinary Optimization* 2014;49(1):1–38. URL: `https://www.scopus.com/inward/record.uri?eid=2-s2.0-84892791680&doi=10.1007%2fs00158-013-0956-z&partnerID=40&md5=fa677158e95f2f851a4efe32974b4ffc`.
7. Acar, E., Bayrak, G., Jung, Y., Lee, I., Ramu, P., Ravichandran, S.. Modeling, analysis, and optimization under uncertainties: a review. *Structural and Multidisciplinary Optimization* 2021;64(5):2909–2945. URL: `https://www.scopus.com/inward/record.uri?eid=2-s2.0-85113170316&doi=10.1007%2fs00158-021-03026-7&partnerID=40&md5=f290f97bc2cdc8aec9b6e851ca63b77d`.
8. Wujek, B., Renaud, J., Batill, S., Brockman, J.. Concurrent subspace optimization using design variable sharing in a distributed computing environment. *Concurrent Engineering Research and Applications* 1996;4(4):361–376. URL: `https://www.scopus.com/inward/record.uri?eid=2-s2.0-0001110621&doi=10.1177%2f1063293x9600400405&partnerID=40&md5=b0e35f498b22e75067a4f95893662ecf`.
9. Mu, X.F., Yao, W.X., Yu, X.Q., Liu, K.L., Xue, F.. Survey of surrogate models used in mdo. *Jisuan Lixue Xuebao/Chinese Journal of Computational Mechanics* 2005;22(5):608–612. URL: `https://www.scopus.com/inward/record.uri?eid=2-s2.0-28244431756&partnerID=40&md5=72b52229fb2cfe4c2b983d1b13c55c75`.
10. Sabido, A., Bahamonde, L., Harik, R., van Tooren, M.. Maturity assessment of the laminate variable stiffness design process. *Composite Structures* 2017;160:804–812. URL: `https://www.scopus.com/inward/record.uri?eid=2-s2.0-85002831694&doi=10.1016%2fj.compstruct.2016.10.081&partnerID=40&md5=6af25579d15e51cafae0ba62bf855e9a`.
11. Afzal, M., Liu, Y., Cheng, J., Gan, V.. Reinforced concrete structural design optimization: A critical review. *Journal of Cleaner Production* 2020;260. URL: `https://www.scopus.com/inward/record.uri?eid=2-s2.0-85082103990&doi=10.1016%2fj.jclepro.2020.120623&partnerID=40&md5=050bc62e4ed71097194299ae986665f5`.
12. Del Grosso, A., Basso, P.. Adaptive building skin structures. *Smart Materials and Structures* 2010;19(12). URL: `https://www.scopus.com/inward/record.uri?eid=2-s2.0-78649933023&doi=10.1088%2f0964-1726%2f19%2f12%2f124011&partnerID=40&md5=b69257bf1a0643629955bce703653e92`.
13. Samareh, J.. Survey of shape parameterization techniques for high-fidelity multidisciplinary

shape optimization. *AIAA Journal* 2001;39(5):877–884. URL: https://www.scopus.com/inward/record.uri?eid=2-s2.0-0035336348&doi=10.2514%2f2.1391&partnerID=40&md5=552ceeabc82602b5a29d8ce7cb6bdad3.

14. Werner, Y., Vietor, T., Weinert, M., Erber, T.. Multidisciplinary design optimization of a generic b-pillar under package and design constraints. *Engineering Optimization* 2021;53(11):1884–1901. URL: https://www.scopus.com/inward/record.uri?eid=2-s2.0-85095731361&doi=10.1080%2f0305215X.2020.1837791&partnerID=40&md5=4ca11b28aea0d92a6668b332d7039510.
15. Sobieszczanski-Sobieski, J., Haftka, R.. Multidisciplinary aerospace design optimization: Survey of recent developments. *Structural Optimization* 1997;14(1):1–23. URL: https://www.scopus.com/inward/record.uri?eid=2-s2.0-0031211068&doi=10.1007%2fBF01197554&partnerID=40&md5=0936960f73e570537f6fd90efd4cab84.
16. Yao, W., Chen, X., Luo, W., Van Tooren, M., Guo, J.. Review of uncertainty-based multidisciplinary design optimization methods for aerospace vehicles. *Progress in Aerospace Sciences* 2011;47(6):450–479. URL: https://www.scopus.com/inward/record.uri?eid=2-s2.0-80052732756&doi=10.1016%2fj.paerosci.2011.05.001&partnerID=40&md5=bd196cf6cd74f2305f8726bd493a5290.
17. Grihon, S.. Structure sizing optimization capabilities at airbus. In: *World Congress of Structural and Multidisciplinary Optimisation*. Springer; 2017:719–737.
18. Iorga, L., Malmedy, V., Stodieck, O., Coggon, S., Loxham, J.. Preliminary sizing optimisation of aircraft structures: Industrial challenges and practices. In: *6th Aircraft Structural Design Conference*. 2019:.
19. Zhang, S., Xia, M., Zhong, B.. Evolution and technical factors influencing civil aircraft aerodynamic configuration. *Hangkong Xuebao/Acta Aeronautica et Astronautica Sinica* 2016;37(1):30–44. URL: https://www.scopus.com/inward/record.uri?eid=2-s2.0-84960412537&doi=10.7527%2fS1000-6893.2015.0311&partnerID=40&md5=40ec7600f306564421d435392f6c49b5.
20. Hu, X., Chen, X., Parks, G., Yao, W.. Review of improved monte carlo methods in uncertainty-based design optimization for aerospace vehicles. *Progress in Aerospace Sciences* 2016;86:20–27. URL: https://www.scopus.com/inward/record.uri?eid=2-s2.0-84990842396&doi=10.1016%2fj.paerosci.2016.07.004&partnerID=40&md5=f2abfd2042fc50357cdd51545e5de500.
21. Ciampa, P., Nagel, B.. Agile paradigm: The next generation collaborative mdo for the development of aeronautical systems. *Progress in Aerospace Sciences* 2020;119. URL: https://www.scopus.com/inward/record.uri?eid=2-s2.0-85090203512&doi=10.1016%2fj.paerosci.2020.100643&partnerID=40&md5=dfab0ebd23894cb6cb994abb98959676.
22. Lefebvre, T., Bartoli, N., Dubreuil, S., Panzeri, M., Lombardi, R., Vecchia, P.D., Stingo, L., Nicolosi, F., Marco, A.D., Ciampa, P., Anisimov, K., Savelyev, A., Mirzoyan, A., Isyanov, A.. Enhancing optimization capabilities using the agile collaborative mdo framework with application to wing and nacelle design. *Progress in Aerospace Sciences* 2020;119. doi:10.1016/j.paerosci.2020.100649.
23. Sferza, M., Ninić, J., Chronopoulos, D., Glock, F., Daoud, F.. Multidisciplinary optimisation of aircraft structures with critical non-regular areas: Current practice and challenges. *Aerospace* 2021;8(8). URL: https://www.scopus.com/inward/record.uri?eid=2-s2.0-85112739163&doi=10.3390%2faerospace8080223&partnerID=40&md5=dadc738132b12e95c3ca3c03d7988a27.
24. Friedmann, P.. Helicopter vibration reduction using structural optimization with aeroelastic/multidisciplinary constraints - a survey. *Journal of Aircraft* 1991;28(1):8–21. URL: https://www.scopus.com/inward/record.uri?eid=2-s2.0-85002976497&doi=10.2514%2f3.45987&partnerID=40&md5=c654d341e926f3c766158aada2522e8c.
25. Bhatia, K.G., Wertheimer, J.. Aeroelastic challenges for a high speed civil transport. pt 6; 1993:3661–3670. URL: https://www.scopus.com/inward/record.uri?eid=2-s2.0-0027190087&partnerID=40&md5=0a50431c2ab74409492eaeac0073d1b7.
26. Taylor, R.. The role of optimization in component structural design: application to the f-35 joint strike fighter. In: *25th International Congress of the Aeronautical Sciences*. 2006:.

27. Cameron, C., Lind, E., Wennhage, P., Göransson, P.. Proposal of a methodology for multidisciplinary design of multifunctional vehicle structures including an acoustic sensitivity study. *International Journal of Vehicle Structures and Systems* 2009;1(1-3):3–15. URL: https://www.scopus.com/inward/record.uri?eid=2-s2.0-84857772404&doi=10.4273%2fijvss.1.1-3.01&partnerID=40&md5=d78e552dbe8a59b275b31fdf9c53a96d.
28. Jonsson, E., Riso, C., Lupp, C., Cesnik, C., Martins, J., Epureanu, B.. Flutter and post-flutter constraints in aircraft design optimization. *Progress in Aerospace Sciences* 2019;109. URL: https://www.scopus.com/inward/record.uri?eid=2-s2.0-85065616673&doi=10.1016%2fj.paerosci.2019.04.001&partnerID=40&md5=a1bb91dafc70c4b43f5d04cfba64c57a.
29. Li, Q., Li, G., Wei, Y., Ran, Y., Wu, B., Tan, G., Li, Y., Chen, S., Lei, B., Xu, Q.. Review of aeroelasticity design for advanced fighter. *Hangkong Xuebao/Acta Aeronautica et Astronautica Sinica* 2020;41(6). URL: https://www.scopus.com/inward/record.uri?eid=2-s2.0-85088018234&doi=10.7527%2fS1000-6893.2019.23430&partnerID=40&md5=de4cb7c98e3af53f35ecc7f7042164f8.
30. Perullo, C., Mavris, D.. A review of hybrid-electric energy management and its inclusion in vehicle sizing. *Aircraft Engineering and Aerospace Technology* 2014;86(6):550–557. URL: https://www.scopus.com/inward/record.uri?eid=2-s2.0-84913552386&doi=10.1108%2fAEAT-04-2014-0041&partnerID=40&md5=af39e356030aeb2a78f946185f6c5e86.
31. Brelje, B., Martins, J.. Electric, hybrid, and turboelectric fixed-wing aircraft: A review of concepts, models, and design approaches. *Progress in Aerospace Sciences* 2019;104:1–19. URL: https://www.scopus.com/inward/record.uri?eid=2-s2.0-85051675367&doi=10.1016%2fj.paerosci.2018.06.004&partnerID=40&md5=f2ee2f103388d5ac5126bfe632d13c70.
32. Okonkwo, P., Smith, H.. Review of evolving trends in blended wing body aircraft design. *Progress in Aerospace Sciences* 2016;82:1–23. URL: https://www.scopus.com/inward/record.uri?eid=2-s2.0-84960172072&doi=10.1016%2fj.paerosci.2015.12.002&partnerID=40&md5=7f8853c29227d7956f974936d941d561.
33. Rodriguez, A.. Morphing aircraft technology survey. vol. 21. 2007:15064–15079. URL: https://www.scopus.com/inward/record.uri?eid=2-s2.0-34250899822&partnerID=40&md5=d640e0a71dceeb8b42233b09bbac1322.
34. Rais-Rohani, M., Dean, E.. Toward manufacturing and cost considerations in multidiscbplinary aircraft design. 1996:2602–2612. URL: https://www.scopus.com/inward/record.uri?eid=2-s2.0-0029699930&doi=10.2514%2f6.1996-1620&partnerID=40&md5=7f07910e0db5f0f13ae9aca6551fcc46.
35. Schuhmacher, G., Daoud, F., Petersson, O., Wagner, M.. Multidisciplinary airframe design optimisation. In: *28th International Congress of the Aeronautical Sciences*; vol. 1. 2012:44–56. URL: https://www.scopus.com/inward/record.uri?eid=2-s2.0-84878589468&partnerID=40&md5=fe55025a939466f36dc16c51aca6011f; cited By 14.
36. Grihon, S.. Structure sizing optimization capabilities at airbus. In: *Advances in Structural and Multidisciplinary Optimization*. 2018:119–126. doi:10.1007/978-3-319-67988-4_55.
37. Iorga, L., Malmedy, V., Stodieck, O., Loxham, J., Coggon, S.. Preliminary sizing optimisation of aircraft structures - industrial challenges and practices. In: *6th Aircraft Structural Design Conference, Bristol*. 2018:.
38. Liersch, C.M., Hepperle, M.. A distributed toolbox for multidisciplinary preliminary aircraft design. *CEAS Aeronautical Journal* 2011;2(1-4):57–68.
39. Daoud, F., Deinert, S., Maierl, R., Petersson, Ö.. Integrated multidisciplinary aircraft design process supported by a decentral MDO framework. In: *16th AIAA/ISSMO Multidisciplinary Analysis and Optimization Conference*. 2015:URL: https://arc.aiaa.org/doi/abs/10.2514/6.2015-3090. doi:10.2514/6.2015-3090. arXiv:https://arc.aiaa.org/doi/pdf/10.2514/6.2015-3090.
40. National Institute for Aviation Research, . Composite Materials Handbook; vol. Polymer Matrix Composites: Materials Usage, Design, and Analysis. SAE International; 2012.
41. Irisarri, F.X., Lasseigne, A., Leroy, F.H., Le Riche, R.. Optimal design of laminated composite structures with ply drops using stacking sequence tables. *Composite Structures* 2014;107:559–

569. URL: https://www.scopus.com/inward/record.uri?eid=2-s2.0-84889642786&doi=10.1016%2fj.compstruct.2013.08.030&partnerID=40&md5=f6afa372183fcd5e73ec54385410335b. doi:10.1016/j.compstruct.2013.08.030; cited By 62.

42. Ntourmas, G., Glock, F., Daoud, F., Schuhmacher, G., Chronopoulos, D., Özcan, E.. Mixed integer linear programming formulations of the stacking sequence and blending optimisation of composite structures. *Composite Structures* 2021;264:113660. URL: https://www.sciencedirect.com/science/article/pii/S0263822321001215. doi:https://doi.org/10.1016/j.compstruct.2021.113660.
43. Vannucci, P., Verchery, G.. A special class of uncoupled and quasi-homogeneous laminates. *Composites Science and Technology* 2001;61(10):1465–1473. URL: https://www.scopus.com/inward/record.uri?eid=2-s2.0-0035421781&doi=10.1016%2fS0266-3538%2801%2900039-2&partnerID=40&md5=e86d8e0b13e7a439f3a9fc28a1df8136. doi:10.1016/S0266-3538(01)00039-2; cited By 46.
44. Montemurro, M.. An extension of the polar method to the first-order shear deformation theory of laminates. *Composite Structures* 2015;127:328–339. URL: https://www.sciencedirect.com/science/article/pii/S026382231500197X. doi:https://doi.org/10.1016/j.compstruct.2015.03.025.
45. Montemurro, M.. The polar analysis of the third-order shear deformation theory of laminates. *Composite Structures* 2015;131:775–789. URL: https://www.sciencedirect.com/science/article/pii/S0263822315004791. doi:https://doi.org/10.1016/j.compstruct.2015.06.016.
46. Raju, G., Wu, Z., Kim, B.C., Weaver, P.M.. Prebuckling and buckling analysis of variable angle tow plates with general boundary conditions. *Composite Structures* 2012;94(9):2961–2970. URL: https://www.sciencedirect.com/science/article/pii/S0263822312001596. doi:https://doi.org/10.1016/j.compstruct.2012.04.002.
47. Montemurro, M., Vincenti, A., Vannucci, P.. Design of the elastic properties of laminates with a minimum number of plies. *Mechanics of Composite Materials* 2012;48:369–390.
48. Montemurro, M., Catapano, A.. A general b-spline surfaces theoretical framework for optimisation of variable angle-tow laminates. *Composite Structures* 2019;209:561–578. URL: https://www.sciencedirect.com/science/article/pii/S0263822318324334. doi:https://doi.org/10.1016/j.compstruct.2018.10.094.
49. Martín, J.C.. Composite optimization techniques for aircraft components structural sizing. In: *8th European Conference for Aeronautics and Space Sciences (EUCASS)*. 2019:doi:10.13009/EUCASS2019-268.
50. Thompson, R.J., Blom-Schieber, A.W.. Sublaminate library generation for optimization of multi-panel composite parts. 2017. URL: https://patents.google.com/patent/US20170228494A1/en.
51. Blom, A.W., Kang, L.S., Epton, M.A.. Ply blending and stacking sequence. 2015. URL: https://patents.google.com/patent/US20170057666A1/en.
52. Coates, T., Smith, A., Emanuel, M., Peterson, B.. Automation of optimal laminate design. *Australian Journal of Mechanical Engineering* 2008;6(2):119–126. doi:10.1080/14484846.2008.11464566.
53. IJsselmuiden, S.. Optimal design of variable stiffness composite structures using lamination parameters. Ph.D. thesis; TU Delft; 2011. URL: https://repository.tudelft.nl/islandora/object/uuid%3A973a564b-5734-42c4-a67c-1044f1e25f1c.
54. Macquart, T., Bordogna, M., Lancelot, P., De Breuker, R.. Derivation and application of blending constraints in lamination parameter space for composite optimisation. *Composite Structures* 2016;135:224–235. URL: https://www.scopus.com/inward/record.uri?eid=2-s2.0-84943657194&doi=10.1016%2fj.compstruct.2015.09.016&partnerID=40&md5=6d3933c752b04a077dcfcaa5b577b939. doi:10.1016/j.compstruct.2015.09.016; cited By 7.
55. Montemurro, M., Pagani, A., Fiordilino, G., Pailhès, J., Carrera, E.. A general multi-scale two-level optimisation strategy for designing composite stiffened panels. *Composite Structures* 2018;201:968–979. URL: https://www.scopus.com/inward/record.uri?eid=2-s2.0-85049726538&doi=10.1016%2fj.compstruct.2018.06.119&partnerID=40&md5=450ce63af0ea858b5673608aae100e30. doi:10.1016/j.compstruct.2018.06.119; cited By 0.

56. Orifici, A., Herszberg, I., Thomson, R.. Review of methodologies for composite material modelling incorporating failure. *Composite Structures* 2008;86:194–210. doi:10.1016/j.compstruct.2008.03.007.
57. Camanho, P., Hallett, S.. Numerical Modelling of Failure in Advanced Composite Materials. Woodhead Publishing Series in Composites Science and Engineering; 2015. ISBN 978-0-08100-342-8.
58. Echaabi, J., Trochu, F., Gauvin, R.. Review of failure criteria of fibrous composite materials. *Polymer Composites* 1996;17:786–798. doi:10.1002/pc.10671.
59. Paris, F., Jackson, K.. A study of failure criteria of fibrous composite materials. *NASA Scientific and Technical Information (STI) Program Office* 2001;:76doi:NASA/CR-2001-210661.
60. Lambe, A., Kennedy, G., Martins, J.. An evaluation of constraint aggregation strategies for wing box mass minimization. *Structural and Multidisciplinary Optimization* 2017;55:257–277. URL: http://dx.doi.org/10.1007/s00158-016-1495-1. doi:10.1007/s00158-016-1495-1.
61. Bach, T., Dähne, S., Heinrich, L., Hühne, C.. Structural optimization of composite wings in an automated multi-disciplinary environment. *AIAA AVIATION 2014 -14th AIAA Aviation Technology, Integration, and Operations Conference* 2014;:1–13doi:10.2514/6.2014-2295.
62. Dávila, C., Camanho, P., Rose, C.. Failure criteria for frp laminates. *Journal of Composite Materials* 2005;39:323–345.
63. Pinho, S., Dávila, C., Camanho, P., Iannucci, L., Robinson, P.. Failure models and criteria for frp under in-plane or three-dimensional stress states including shear non-linearity. *Nasa/Tm-2005-213530* 2005;:68doi:NASA/TM-2005-213530.
64. Catalanotti, G., Camanho, P., Marques, A.. Three-dimensional failure criteria for fiber-reinforced laminates. *Composite Structures* 2013;95:63–79. URL: http://dx.doi.org/10.1016/j.compstruct.2012.07.016. doi:10.1016/j.compstruct.2012.07.016.
65. Camanho, P., Arteiro, A., Catalanotti, G., Melro, A., Vogler, M.. Three-dimensional invariant-based failure criteria for transversely isotropic fibre-reinforced composites. 2015. URL: http://dx.doi.org/10.1016/B978-0-08-100332-9.00005-0. doi:10.1016/B978-0-08-100332-9.00005-0.
66. Aminpour, M., Shin, Y., Sues, R., WU, Y.T.. A framework for reliability-based mdo of aerospace systems. 2002:1–10.
67. Reinoso, J., Blázquez, A., Estefani, A., París, F., Cañas, J., Arévalo, E., Cruz, F.. Experimental and three-dimensional global-local finite element analysis of a composite component including degradation process at the interfaces. *Composites Part B: Engineering* 2012;43:1929–1942. URL: http://dx.doi.org/10.1016/j.compositesb.2012.02.010. doi:10.1016/j.compositesb.2012.02.010.
68. Akterskaia, M., Camanho, P., Jansen, E., Arteiro, A., Rolfes, R.. Progressive delamination analysis through two-way global-local coupling approach preserving energy dissipation for single-mode and mixed-mode loading. *Composite Structures* 2019;223:110892. URL: https://doi.org/10.1016/j.compstruct.2019.110892. doi:10.1016/j.compstruct.2019.110892.
69. Albert, C., Fernlund, G.. Spring-in and warpage of angled composite laminates. *Composites Science and Technology* 2002;62(14):1895–1912. doi:https://doi.org/10.1016/S0266-3538(02)00105-7.
70. Traiforos, N., Turner, T., Runeberg, P., Fernass, D., Chronopoulos, D., Glock, F., Schuhmacher, G., Hartung, D.. A simulation framework for predicting process-induced distortions for precise manufacturing of aerospace thermoset composites. *Composite Structures* 2021;275:114465. URL: https://www.sciencedirect.com/science/article/pii/S0263822321009272. doi:https://doi.org/10.1016/j.compstruct.2021.114465.
71. Piperni, P., DeBlois, A., Henderson, R.. Development of a multilevel multidisciplinary-optimization capability for an industrial environment. *AIAA Journal* 2013;51(10):2335–2352. doi:10.2514/1.J052180.
72. Taylor, R.M.. The role of optimization in component structural design: application to the f-35 joint strike fighter. In: *25th International Congress of the Aeronautical Sciences*. 2006:URL: https://www.icas.org/ICAS_ARCHIVE/ICAS2006/ABSTRACTS/198.HTM.
73. Noevere, A.T., Wilhite, A.W.. Bi-Level Optimization of a Conceptual Metallic Wing Box with Stiffness Constraints. In: *57th AIAA/ASCE/AHS/ASC Structures, Structural Dynamics, and Ma-*

terials Conference. American Institute of Aeronautics and Astronautics; 2016:URL: https://arc.aiaa.org/doi/abs/10.2514/6.2016-0235. doi:10.2514/6.2016-0235.

74. Locatelli, D., Tamijani, A.Y., Mulani, S.B., Liu, Q., Kapania, R.K.. Multidisciplinary Optimization of Supersonic Wing Structures Using Curvilinear Spars and Ribs (SpaRibs). In: *54th AIAA/ASME/ASCE/AHS/ASC Structures, Structural Dynamics, and Materials Conference*. American Institute of Aeronautics and Astronautics; 2013:URL: https://arc.aiaa.org/doi/abs/10.2514/6.2013-1931. doi:10.2514/6.2013-1931; _eprint: https://arc.aiaa.org/doi/pdf/10.2514/6.2013-1931.
75. Liu, Q., Mulani, S.B., Kapania, R.K.. Global/Local Multidisciplinary Design Optimization of Subsonic Wing. In: *10th AIAA Multidisciplinary Design Optimization Conference*. AIAA SciTech Forum; American Institute of Aeronautics and Astronautics; 2014:URL: https://arc.aiaa.org/doi/10.2514/6.2014-0471. doi:10.2514/6.2014-0471.
76. Liu, Q., Jrad, M., Mulani, S.B., Kapania, R.K.. Integrated Global Wing and Local Panel Optimization of Aircraft Wing. In: *56th AIAA/ASCE/AHS/ASC Structures, Structural Dynamics, and Materials Conference*. American Institute of Aeronautics and Astronautics; 2015:URL: https://arc.aiaa.org/doi/abs/10.2514/6.2015-0137. doi:10.2514/6.2015-0137.
77. Liu, Q., Jrad, M., Mulani, S.B., Kapania, R.K.. Global/Local Optimization of Aircraft Wing Using Parallel Processing. *AIAA Journal* 2016;54(11):3338–3348. URL: https://doi.org/10.2514/1.J054499. doi:10.2514/1.J054499.
78. Robinson, J., Doyle, S., Ogawa, G., Baker, M., De, S., Jrad, M., Kapania, R.. Aeroservoelastic Optimization of Wing Structure Using Curvilinear Spars and Ribs (SpaRibs). 2016:doi:10.2514/6.2016-3994.
79. Stanford, B.K., Jutte, C.V., Coker, C.A.. Aeroelastic Sizing and Layout Design of a Wingbox Through Nested Optimization. *AIAA Journal* 2019;57(2):848–857. URL: https://arc.aiaa.org/doi/10.2514/1.J057428. doi:10.2514/1.J057428.
80. Stanford, B.. Shape, sizing, and topology design of a wingbox under aeroelastic constraints. vol. 1 PartF. 2020:1–11. URL: https://www.scopus.com/inward/record.uri?eid=2-s2.0-85092922814&doi=10.2514%2f6.2020-3147&partnerID=40&md5=e39273222e812c78c0dc4557302e375f. doi:10.2514/6.2020-3147.
81. Guyan, R.J.. Reduction of stiffness and mass matrices. *AIAA Journal* 1965;3(2):380–380. doi:10.2514/3.2874.
82. Setoodeh, S., Abdalla, M., Gürdal, Z.. Approximate feasible regions for lamination parameters. vol. 2. 2006:814–822. URL: https://www.scopus.com/inward/record.uri?eid=2-s2.0-33846551299&partnerID=40&md5=fe2ce34c2765af5268ff171dd4d32ee3; cited By 32.
83. Liu, X., Featherston, C.A., Kennedy, D.. Two-level layup optimization of composite laminate using lamination parameters. *Composite Structures* 2019;211:337 – 350. URL: http://www.sciencedirect.com/science/article/pii/S0263822318325753. doi:https://doi.org/10.1016/j.compstruct.2018.12.054.
84. Montemurro, M., Vincenti, A., Vannucci, P.. A two-level procedure for the global optimum design of composite modular structures—application to the design of an aircraft wing part i. *Journal of Optimization Theory and Applications* 2012;155(1):1–23. URL: https://doi.org/10.1007/s10957-012-0067-9. doi:10.1007/s10957-012-0067-9.
85. Ntourmas, G., Glock, F., Daoud, F., Schuhmacher, G., Chronopoulos, D., Özcan, E.. Generic stacks and application of composite rules for the detailed sizing of laminated structures. *Composite Structures* 2021;276:114487. URL: https://www.sciencedirect.com/science/article/pii/S0263822321009491. doi:https://doi.org/10.1016/j.compstruct.2021.114487.
86. Meddaikar, Y., Irisarri, F.X., Abdalla, M.. Laminate optimization of blended composite structures using a modified shepard's method and stacking sequence tables. *Structural and Multidisciplinary Optimization* 2017;55(2):535–546. URL: https://www.scopus.com/inward/record.uri?eid=2-s2.0-84976430839&doi=10.1007%2fs00158-016-1508-0&partnerID=40&md5=71b242db19c52d820946b5dcdf3aee3f. doi:10.1007/s00158-016-1508-0; cited By 3.

87. Jing, Z., Fan, X., Sun, Q.. Global shared-layer blending method for stacking sequence optimization design and blending of composite structures. *Composites Part B: Engineering* 2014;69:181–190. URL: https://www.scopus.com/inward/record.uri?eid=2-s2.0-84908378880&doi=10.1016%2fj.compositesb.2014.09.039&partnerID=40&md5=1a4c816ef5429bb7b59ea1566fbad64b. doi:10.1016/j.compositesb.2014.09.039; cited By 16.
88. Picchi Scardaoni, M., Montemurro, M., Panettieri, E., Catapano, A.. New blending constraints and a stack-recovery strategy for the multi-scale design of composite laminates. *Structural and Multidisciplinary Optimization* 2020;doi:https://doi.org/10.1007/s00158-020-02725-x.
89. Tsai, S., Melo, J., Sihn, S., Arteiro, A., Rainsberger, R.. Composite Laminates: Theory and Practice of Analysis, Design and Automated Layup. Stanford Aeronautics & Astronautics; 2017. ISBN 9780986084539.
90. Tsai, S., Melo, J.. An invariant-based theory of composites. *Composites Science and Technology* 2014;100:237–243. URL: http://dx.doi.org/10.1016/j.compscitech.2014.06.017. doi:10.1016/j.compscitech.2014.06.017.
91. Bramsiepe, K.R., Handojo, V., Meddaikar, M., Schulze, M., Klimmek, T.. Loads and structural optimisation process for composite long range transport aircraft configuration. *2018 Multidisciplinary Analysis and Optimization Conference* 2018;:1–20doi:10.2514/6.2018-3572.
92. Ijsselmuiden, S., Abdalla, M., Gürdal, Z.. Implementation of strength-based failure criteria in the lamination parameter design space. *AIAA Journal* 2008;46:1826–1834. doi:10.2514/1.35565.
93. Tsai, S., Melo, J.. A unit circle failure criterion for carbon fiber reinforced polymer composites. *Composites Science and Technology* 2016;123:71–78. doi:10.1016/j.compscitech.2015.12.011.
94. Corrado, G., Arteiro, A., Marques, A., Reinoso, J., Daoud, F., Glock, F.. An extended invariant approach to laminate failure of fibre-reinforced polymer structures. *The Aeronautical Journal* 2021;:1–24URL: https://doi.org/10.1017/aer.2021.121. doi:https://doi.org/10.1017/aer.2021.121.
95. Vermes, B., Tsai, S.W., Riccio, A., Caprio, F.D., Roy, S.. Application of the tsai's modulus and double-double concepts to the definition of a new affordable design approach for composite laminates. *Composite Structures* 2020;:113246URL: https://doi.org/10.1016/j.compstruct.2020.113246. doi:10.1016/j.compstruct.2020.113246.
96. Molker, H., Gutkin, R., Pinho, S., Asp, L.. Hot spot analysis in complex composite material structures. *Composite Structures* 2019;207:776–786. URL: https://doi.org/10.1016/j.compstruct.2018.09.088. doi:10.1016/j.compstruct.2018.09.088.
97. Zou, X., Yan, S., Reza, M., Brown, L., Jones, A.. An abaqus plugin for efficient damage initiation hotspot identification in large-scale composite structures with repeated features. *Advances in Engineering Software* 2021;153:102964. URL: https://doi.org/10.1016/j.advengsoft.2020.102964. doi:10.1016/j.advengsoft.2020.102964.
98. Molker, H., Gutkin, R., Asp, L.. Implementation of failure criteria for transverse failure of orthotropic non-crimp fabric composite materials. *Composites Part A* 2017;92:158–166. URL: http://dx.doi.org/10.1016/j.compositesa.2016.09.021. doi:10.1016/j.compositesa.2016.09.021.
99. Dávila, C., Rose, C., Iarve, E.. Modeling fracture and complex crack networks in laminated composites. 2013:297–347. doi:10.1142/9781848167858_0008.
100. Furtado, C., Catalanotti, G., Arteiro, A., Gray, P., Wardle, B., Camanho, P.. Simulation of failure in laminated polymer composites: Building-block validation. *Composite Structures* 2019;226:111168. URL: https://doi.org/10.1016/j.compstruct.2019.111168. doi:10.1016/j.compstruct.2019.111168.
101. Zhuang, F., Arteiro, A., Furtado, C., Chen, P., Camanho, P.. Mesoscale modelling of damage in single- and double-shear composite bolted joints. *Composite Structures* 2019;226. doi:10.1016/j.compstruct.2019.111210.
102. Turon, A., Dávila, C., Camanho, P., Costa, J.. An engineering solution for mesh size effects in the simulation of delamination using cohesive zone models. *Engineering Fracture Mechanics* 2007;74(10):1665–1682. doi:10.1016/j.engfracmech.2006.08.025.
103. Svanberg, J.M.. Predictions of manufacturing induced shape distortions. Lulea University of Tech-

nology; 2002:.

104. Kappel, E., Stefaniak, D., Hühne, C.. Process distortions in prepreg manufacturing – an experimental study on cfrp l-profiles. *Composite Structures* 2013;106:615–625. doi:http://dx.doi.org/10.1016/j.compstruct.2013.07.020.

105. Fernlund, G., Rahman, N., Courdji, R., Bresslauer, M., Poursartip, A., Willden, K., Nelson, K.. Experimental and numerical study of the effect of cure cycle, tool surface, geometry, and lay-up on the dimensional fidelity of autoclave-processed composite parts. *Composites Part A: Applied Science and Manufacturing* 2002;33(3):341–351. doi:https://doi.org/10.1016/S1359-835X(01)00123-3.

106. Wisnom, M., Gigliotti, M., Ersoy, N., Campbell, M., Potter, K.. Mechanisms generating residual stresses and distortion during manufacture of polymer–matrix composite structures. *Composites Part A: Applied Science and Manufacturing* 2006;37(4):522–529. doi:https://doi.org/10.1016/j.compositesa.2005.05.019; internal Stresses in Polymer Composites.

107. Kappel, E.. Forced-interaction and spring-in – relevant initiators of process-induced distortions in composite manufacturing. *Composite Structures* 2016;140:217—229. doi:http://dx.doi.org/10.1016/j.compstruct.2016.01.016.

108. Stefaniak, D., Kappel, E., Spröwitz, T., Hühne, C.. Experimental identification of process parameters inducing warpage of autoclave-processed cfrp parts. *Composites Part A: Applied Science and Manufacturing* 2012;43(7):1081—-1091. doi:http://dx.doi.org/10.1016/j.compositesa.2012.02.013.

109. Kitselis, A., Traiforos, N., Manolakos, D.. The effect of resonance on the void content in cfrp tubes. *Composites Part B: Engineering* 2016;106:164–171. URL: https://www.sciencedirect.com/science/article/pii/S1359836816318777. doi:https://doi.org/10.1016/j.compositesb.2016.09.019.

110. Potter, K., Langer, C., Hodgkiss, B., Lamb, S.. Sources of variability in uncured aerospace grade unidirectional carbon fibre epoxy preimpregnate. *Composites Part A: Applied Science and Manufacturing* 2007;38(3):905 – 916. doi:https://doi.org/10.1016/j.compositesa.2006.07.010.

111. Lightfoot, J.S., Wisnom, M.R., Potter, K.. A new mechanism for the formation of ply wrinkles due to shear between plies. *Composites Part A: Applied Science and Manufacturing* 2013;49:139–147. URL: https://www.sciencedirect.com/science/article/pii/S1359835X13000730. doi:https://doi.org/10.1016/j.compositesa.2013.03.002.

112. Lamers, E.. Shape distortions in fabric reinforced composite products due to processing induced fibre reorientation. Ph.D. thesis; Netherlands; 2004.

113. Fernlund, G., Osooly, A., Poursartip, A., Vaziri, R., Courdji, R., Nelson, K., George, P., Hendrickson, L., Griffith, J.. Finite element based prediction of process-induced deformation of autoclaved composite structures using 2d process analysis and 3d structural analysis. *Composite Structures* 2003;62(2):223—234. doi:https://doi.org/10.1016/S0263-8223(03)00117-X.

114. Zhang, J., Zhang, M., Li, S., Pavier, M., Smith, D.. Residual stresses created during curing of a polymer matrix composite using a viscoelastic model. *Composites Science and Technology* 2016;130:20–27. doi:http://dx.doi.org/10.1016/j.compscitech.2016.05.002.

115. Benavente, M., Marcin, L., Courtois, A., Lévesque, M., Ruiz, E.. Numerical analysis of viscoelastic process-induced residual distortions during manufacturing and post-curing. *Composites Part A: Applied Science and Manufacturing* 2018;107:205—-216. doi:https://doi.org/10.1016/j.compositesa.2018.01.005.

116. Ding, A., Li, S., Sun, J., Wanga, J., Zu, L.. A thermo-viscoelastic model of process-induced residual stresses in composite structures with considering thermal dependence. *Composite Structures* 2016;136:34–43. doi:http://dx.doi.org/10.1016/j.compstruct.2015.09.014.

117. Poon, H., Ahmad, M.F.. A material point time integration procedure for anisotropic, thermo rheologically simple, viscoelastic solids. *Computational Mechanics* 1998;21(3):236–242. doi:https://doi.org/10.1007/s004660050298.

118. Bogetti, T.A., Gillespie, J.W.. Process-induced stress and deformation in thick-section thermoset composite laminates. *Journal of Composite Materials* 1992;26(5):626–660. doi:https://doi.org/10.1177/002199839202600502.

119. Zeng, X., Raghavan, J.. Role of tool-part interaction in process-induced warpage of autoclave-manufactured composite structures. *Composites Part A: Applied Science and Manufacturing* 2010;41:1174—1183. doi:https://doi.org/10.1016/j.compositesa.2010.04.017.
120. Niu, M.C.Y.. Airframe Structural Design - Practical Design Information and Data on Aircraft Structures. 2 ed.; Hong Kong; 1999. ISBN 978-962-7128-09-0. URL: https://app.knovel.com/web/toc.v/cid:kpCASPDID8/viewerType:toc/root_slug:composite-airframe-structures/url_slug:composite-airframe-structures?b-q=compositeairframestructureniu&sort_on=default&b-subscription=true&b-group-by=true&b-sort-on=default&.
121. Hinton, M., Kaddour, A.. Triaxial test results for fibre-reinforced composites: The Second World-Wide Failure Exercise benchmark data. *Journal of Composite Materials* 2013;47(6-7):653–678. URL: https://doi.org/10.1177/0021998312459782. doi:10.1177/0021998312459782.
122. Hinton, M., Kaddour, A., Soden, P.. Failure Criteria in Fibre Reinforced Polymer Composites: The World-Wide Failure Exercise. 2004. ISBN 0080426999.
123. Hinton, M., Kaddour, A.. Triaxial test results for fibre-reinforced composites: The Second World-Wide Failure Exercise benchmark data. *Journal of Composite Materials* 2013;47(6-7):653–678. URL: https://doi.org/10.1177/0021998312459782. doi:10.1177/0021998312459782.
124. Camanho, P., Dávila, C.. Mixed-Mode Decohesion Finite Elements in for the Simulation Composite of Delamination Materials. *Nasa* 2002;TM-2002-21(June):1–37. URL: https://ntrs.nasa.gov/citations/20020053651. doi:10.1177/002199803034505.
125. Johnston, A.A.. An integrated model of the development of process-induced deformation in autoclave processing of composite structures. Ph.D. thesis; University of British Columbia; 1997. doi:http://dx.doi.org/10.14288/1.0088805.